

Characterization of the hydrological and hydrochemical contribution of the North Andean calcareous massifs to the Andean tributaries of the Amazon River (Marañon and Huallaga rivers) through the study of two karstic resurgences:

A comparative study of the hydrology and the hydrochemistry of the resurgences of Palestina and Soloco

Fabien RENOUE, Septembre 2013

Tuteurs : Jean-Loup GUYOT (IRD Pérou, ORE HYBAM)

William SANTINI (IRD Pérou, ORE HYBAM)

James APAESTEGUI (Doctorant UFF, LMI Paleotracés)

ACKNOWLEDGMENTS

First, I would like to thank a lot Jean-Loup GUYOT, for offering me this very (very) interesting internship in the IRD. Thank you for your supervision, all your advices, and for the time you gave me. But especially, thank you for transmitting me your passion for the study of the Andean karsts !

I also would like to thank my other two tutors, William SANTINI and James APAESTEGUI for their supervision, their advices, and for the good times spent together during the field missions.

Thank you to Christelle LAGANE of the GET Laboratory of Toulouse for the analysis of the samples of water, and Jean-Sébastien MOQUET for his explications on the calculation of the karstic ablation rate.

Thank you very much to Claudia VARGAS and the municipality of Nueva Cajamarca for the help they brought to me during my second field campaign in the massif of the Alto Mayo in June. Thank you to Ronald and Lizseth for guiding me during these three weeks of work...and teaching me how to drive a moto ! Thank you also to Anthony for

Finally, thank you to all my mates and colleagues of the “Casita Verde”: Sergio, Jhan Carlo, Hans,... for keeping me company during the large days of work, and to all the staff of the IRD for their kindness and their disponibility: Liliana LALONDE, Sacy NADARADJANE, Miriam SOTO and Alain CORDE.

AGRADECIMIENTOS

Yo quisiera primero agradecer mucho a Jean-Loup GUYOT, por haber ofrecido me está muy (muy) interesante pasantía en el IRD. Gracias por tu supervisión, todos tus consejos, y para el tiempo que me dedicaste. Pero sobre todo, gracias por haber transmitirme tu pasión por el estudio de los karsts andinos.

Yo quisiera también agradecer a mis dos otros tutores, William SANTINI y James APAESTEGUI por su supervisión, sus consejos y por los buenos momentos que pasamos durante los campos de terreno.

Gracias a Christelle LAGANE del laboratorio GET de Toulouse por la análisis de las muestras de agua, y Jean-Sébastien MOQUET por su explicación sobre el cálculo de la tasa de ablación kárstica.

Muchas gracias a Claudia VARGAS y a la municipalidad de Nueva Cajamarca por su ayuda durante mi segunda misión de terreno (en solitario) en el macizo del Alto Mayo. Gracias a Ronald y Lizabeth por haber sido mis guías durante estas tres semanas de trabajo...y por haber aprendido me a manejar una moto ! Gracias también a Anthony por haber servido me de chófer.

Por fin, gracias a todos mis amigos y colegas de la “Casita Verde”: Sergio, Jhan Carlo, Hans,... por haber hecho me compañía a lo largo de mi pasantía y durante los largos días de trabajo, y a todo el equipo del IRD por su amabilidad y su disponibilidad: Liliana LALONDE, Sacy NADARADJANE, Miriam SOTO y Alain CORDE.

REMERCIEMENTS

Je tiens tout d’abord à remercier grandement Jean-Loup GUYOT, pour m’avoir proposé ce stage très (très) intéressant à l’IRD. Merci pour ton encadrement, tes conseils et le temps que tu m’as consacré. Mais surtout, merci pour m’avoir transmis ta passion pour l’étude des karsts andins !

J’aimerais aussi remercier mes deux autres tuteurs, William SANTINI et James APAESTEGUI pour leur encadrement, leurs conseils, et pour tous les bons moments passés ensemble lors des missions de terrain.

Merci à Christelle LAGANE du laboratoire GET de Toulouse pour les analyses des échantillons d’eau, et Jean-Sébastien MOQUET pour ses conseils pour le calcul de l’ablation en milieu karstique.

Un grand merci à Claudia VARGAS et à la municipalité de Nueva Cajamarca pour l’aide qu’ils m’ont apporté durant ma seconde mission de terrain (en solo) dans le massif de l’Alto Mayo. Merci à Ronald et Lizabeth pour m’avoir servi de guides durant ces trois semaines de travail...et pour m’avoir appris à conduire une moto ! Merci aussi à Anthony pour m’avoir servi de chauffeur tout au long de cette mission.

Enfin, merci à mes amis et collègues de la “Casita Verde” : Sergio, Jhan Carlo, Hans,... pour m’avoir tenu compagnie tout au long de mon stage et pendant les longues journées de travail, ainsi qu’à toute l’équipe de l’IRD pour leur gentillesse et leur disponibilité : Liliana LALONDE, Sacy NADARADJANE, Miriam SOTO et Alain CORDE.

TABLE OF CONTENTS

Acknowledgments	I
Agradecimientos	I
Remerciements	II
Table of contents	III
List of figures	V
List of tables	VI
List of abbreviations	VII
Abstract	VIII
Resumen	VIII
Résumé	IX
Introduction	1
Chapter 1. The karsts of the massif of Soloco and of the massif of the Alto Mayo: presentation of the two resurgences studied	3
1. Geographic context	3
1.1. Climatic context	4
1.2. The karstic systems	7
1.2.1. Palestina.....	7
1.2.1.1. Geology of the catchment.....	7
1.2.1.2. Karstic morphology of the Alto Mayo.....	8
1.2.2. Soloco	9
1.2.2.1. Geology of the catchment.....	9
1.2.2.2. Karstic morphology of the massif of Soloco	11
1.3. A first overview of the hydrogeology of the two resurgences	11
1.3.1. Resurgence of Palestina	11
1.3.2. Resurgence of Soloco	11
Chapter 2. The resurgences of Soloco and Palestina: acquisition and treatment of data 12	
1. Acquisition of hydrological and physical chemistry parameters	12
1.1. Treatment of data	13
1.1.1. Recuperation of data	13
1.1.2. Treatment of data	13
1.1.2.1. Resurgence of Soloco	14
1.1.2.2. Resurgence of Palestina.....	16
1.1.3. Monitoring of the hydrogeochemical tracers	22
Chapter 3. Study of the hydrogeological behavior of the two resurgences	23
1. Comparison of the hydrological behavior	23

1.1. Analysis of the flood hydrographs	23
1.2. Correlative analysis.....	24
1.2.1. Generality and methods of analysis	24
1.2.1.1. Crossed analysis	24
1.2.1.2. Simple analysis.....	24
1.2.2. Results.....	25
2. Geochemical characterization of the resurgences.....	27
2.1. Chemistry of the waters	26
2.2. Behavior of the resurgence of Palestina	30
2.3. Behavior of the resurgence of Soloco.....	33
Chapter 4. Hydrogeological contribution of the Andean calcareous massifs to the Andean tributaries of the Amazon: balance of exported dissolved solids and calculation of the karstic ablation rate for the two catchments.....	36
1. Balance of exported dissolved solids	36
2. Calculation of the karstic ablation rate.....	39
Chapter 5. A first overview of the hydrogeology of the massif of the Alto Mayo	42
1. Methods.....	42
2. Results	42
2.1. Hydrology and physical chemistry monitoring of the resurgences.....	42
2.2. Speleological exploration	45
Conclusion.....	47
Bibliography	49
Appendices	51

LIST OF FIGURES

Figure 1: Localization of the resurgences of Soloco (SOL) and Palestina (PAL) (source: Moquet, 2011, modified).....	3
Figure 2: Monthly rainfall: a) at the station of Rioja (X:-6.033 S, Y:-77.167 W, Z: 848 m a.s.l.); b) at the station of Chachapoyas (X:-6.205 S, Y:-77.867 W, Z: 2334 m a.s.l.)	5
Figure 3: a) Altitudinal pluviometric gradient; b) Altitudinal temperature gradient for the areas of Rioja and Chachapoyas (source: Guyot, 2004)	6
Figure 4: Theoretical catchment of the resurgence of Palestina	8
Figure 5: Theoretical catchment of the resurgence of Soloco.....	10
Figure 6: Water levels of the Rio Soloco (Resurgence of Soloco)	14
Figure 7: a) staff gage and CTD water levels registered at the resurgence of Soloco; b) relation between the discharge and the CTD water levels of the resurgence of Soloco.	15
Figure 8: Calibration curve of the resurgence of Soloco (Rio Soloco).....	16
Figure 9: Levels observed on R1 and R2 at Palestina.....	17
Figure 10: First calibration curve of the resurgence of Palestina (Río Jordán).....	18
Figure 11: Relation between the levels measured on R2 and the levels registered by the CTD2 at Palestina	18
Figure 12: Relation between the levels measured on R1 and the levels registered by the CTD1 at Palestina.....	19
Figure 13: Water levels expressed in the referential of R2 at Palestina.....	19
Figure 14: Readjustment of the levels registered by the CTD 1 before the 15/09/2011	20
Figure 15: New serie of water levels in the referential of R2 at Palestina.....	20
Figure 16: New calibration curve of the resurgence of Palestina (Río Jordán)	22
Figure 17: Flood hydrograph: a) Resurgence of Palestina; b) Resurgence of Soloco	23
Figure 18: a) Rainfall-Discharge cross correlograms for the two resurgences; b) Discharge correlograms for the two resurgences	26
Figure 19: Piper diagram for the two resurgences	28
Figure 20: $\text{Ca}^{2+} + \text{Mg}^{2+}$ (meq/L) vs. HCO_3^- (meq/L) graph; b) $\text{Ca}^{2+} + \text{Mg}^{2+}$ (meq/L) vs. $\text{HCO}_3^- + \text{SO}_4^{2-}$ (meq/L) graph.....	28
Figure 21: graph Na^+ vs. Cl^- for the two resurgences	29
Figure 22: Temporal variation of discharge, EC and temperature of the water at the resurgence of Palestina from the 19/05/2011 to the 07/02/2013	31

Figure 23: Zoom from the Figure 21 on the flood event running from the 26/02/2012 to the 02/03/2013.....	32
Figure 24: Temporal variation of water level and temperature of the water at the resurgence of Soloco from the 25/07/12 to the 25/09/12.....	34
Figure 25: Zoom from Figure 23 on the flood event running from the 16/07/12 to the 31/07/12.....	34
Figure 26: Localization of the Andean calcareous massifs. PAL: resurgence of Palestina; SOL: resurgence of Soloco; BOR: HYBAM gaging station of Borja; CHA: HYBAM gaging station of Chazuta (source: Moquet, 2011, modified).....	38
Figure 27: Karstic ablation rate for different climatic contexts according to annual rainfall ..	40
Figure 28: relation between the EC measured and the TDS at Soloco and Palestina	44

LIST OF TABLES

Table 1: resurgences studied in the framework of this internship.....	4
Table 2: Name of the resurgence, with the equipment in place, parameters measured, the monitoring time step, the accuracy of each equipment, and the available data.	12
Table 3: Chronology of the functioning of the equipments of the resurgence of Palestina.	16
Table 4: Stream gagings realized at the resurgence of Palestina.	21
Table 5: Physical chemistry parameters of the two resurgences.....	27
Table 6: Interannual fluxes of dissolved elements and total dissolved solids (i.e. anions+cations+SiO ₂) (TDS _{tot}) for the different stations..	37
Table 7: Net and relative contribution of Soloco, Palestina, and the North Andean calcareous massifs to the Marañon, the Huallaga, the Peruvian Amazon ad the whole Amazon in terms of fluxes of dissolved solids and discharge..	39
Table 8: Ablation rate of the two catchments studied.....	40
Table 9: Values of discharge, electrical conductivity and temperature of water of all the resurgences monitored during the HYBAM-Paleotracés field campaign of June-July 2013..	43
Table 10: estimation of the TDS exported by the resurgences monitored during the HYBAM-PALEOTRACES field campaign of June-July 2013.	45
Table 11: caves found during the HYBAM-PALEOTRACES field campaign of June-July 2013.....	46

LIST OF ABBREVIATIONS

CESPE: Centre d'Explorations Souterraines du Pérou

ECA: Espeleo Club Andino de Lima

GBPE: Grupo Bambuí de Pesquisas Espeleológicas

GSBM : Groupe Spéléo Bagnols Marcoule

INGEMMET: INstituto GEológico Minero y METalúrgico

IRD: Institut de Recherche pour le Développement

HYBAM : HydroGéodynamique du Bassin Amazonien

SENAMHI: SErvicio NAcional de Meteorología e Hidrología

UNALM: Universidad Nacional Agraria de La Molina

ABSTRACT

In the North Peru, the numerous calcareous massifs represent an important source of supply of dissolved elements to the Amazon River. Moreover, thanks to the abundant rainfall in this region, these massifs constitute a water resource no negligible for the populations living at proximity.

The study of these massifs has begun in 2005 thanks to the HYBAM (Hydrogeodynamics of the Amazon Basin) and PALEOTRACES programs led by the French Institute of Research for the Development (IRD). In the framework these programs, a monitoring of the North Peruvian resurgences of Soloco (located in the Oriental Cordillera) and Palestina (located in the Amazonian Piedmont) is respectively realized since 2005 and 2011.

The hydrological comparative study allowed highlighting a very fast response at a rainfall event for the karst of Palestina while the karst of Soloco has a more inertial behavior due to important water reserves. The geochemistry of groundwaters is mainly controlled by the dissolution of limestones and dolomites, and concentrations abnormally high of Na^+ and Cl^- were highlighted at both resurgences. The resurgence of Palestina presents a “piston flow” behavior while a dilution of the waters of the saturated zone by infiltrations waters is observed at Soloco during flood events. At the scale of the High Marañón basin, the North Andean calcareous massifs export each year around 7462.10^3 tons of dissolved solids, which represents 70% of the flux exported by the High Marañón and the Huallaga. The ablation rate was estimated at about 70 mm.Kyr^{-1} for the karst of Soloco, and 53 mm.Kyr^{-1} for the karst of Palestina. These values confirm a global trend which shows that the runoff is the main control factor of ablation.

RESUMEN

En el Norte del Perú, los numerosos macizos calcáreos representan una fuente importante de aporte en elementos disueltos al Amazon. Además, gracias a las abundantes lluvias en esta región, estos macizos constituyen recursos hídricos nada despreciables para las poblaciones viviendo en los alrededores.

El estudio de estos macizos empezó en 2005 gracias a los proyectos HYBAM (Hidrología y Bioquímica de la cuenca Amazónica) y PALEOTRACES llevados por el

Instituto Francés de Investigación para el Desarrollo (IRD). Dentro de estos proyectos, un seguimiento de las resurgencias Norte Peruanas de Soloco (localizada en la Cordillera Oriental) y Palestina (localizada en el piedemonte Amazónico) está llevado desde respectivamente el año 2005 y el año 2011.

El estudio comparativo hidrológico permitió evidenciar una respuesta muy rápida a un evento de lluvia por el karst de Palestina mientras el karst de Soloco presenta un comportamiento más inercial debido a importantes reservas de agua. La geoquímica de las aguas subterráneas esta principalmente controlada por la disolución de las calizas y dolomitas, y concentraciones anormalmente altas de Na y Cl fue evidenciada en las dos resurgencias. La resurgencia de Palestina presenta un comportamiento de tipo “flujo pistón”, mientras se observa a Soloco una dilución de las aguas de la zona saturada por las aguas infiltradas durante los eventos de crecida. A la escala de la cuenca del río Alto Marañón, los macizos calcáreos Norte Andinos exportan cada año unas 7462.10^3 toneladas de elementos disueltos, lo que representa 70% del flujo exportado por el Alto Marañón y el Huallaga. La tasa de ablación fue estimada a 70 mm.Kyr^{-1} por el karst de Soloco, y 53 mm.Kyr^{-1} por el karst de Palestina. Estos valores confirman una tendencia mundial que muestra que la lluvia anual es el principal factor de la erosión

RESUME

Dans le Nord du Pérou, les nombreux massifs calcaires représentent une source importante en termes d'apports en éléments dissous. En outre, de par l'abondance des pluies dans ces régions, ces massifs constituent une ressource en eau non négligeable pour les populations vivant à proximité.

L'étude de ces massifs a débuté en 2005 au travers des programmes HYBAM (Hydro Géodynamique du Bassin Amazonien) et PALEOTRACES conduits par l'Institut de Recherche pour le Développement (IRD). Dans le cadre de ces programmes, un suivi des résurgences de Soloco (située dans la Cordillère Orientale) et Palestina (située dans le Piedmont Amazonien) est réalisé respectivement depuis 2005 et 2011.

L'étude comparative de l'hydrologie des deux résurgences a permis de mettre en évidence une réponse très rapide du karst de Palestina suite à un évènement pluvieux, alors que le karst de Soloco présente un comportement plus inertiel, avec un signal de pluie très filtré dû à d'importantes réserves en eau. La géochimie des eaux souterraines est principalement régie par la dissolution des calcaires et dolomies, et des

concentrations anormalement élevées en Na et Cl ont été mis en évidence au niveau des deux résurgences. Le système de Palestina présente un comportement de type “écoulement piston” alors qu’une dilution des eaux de la zone saturée par les eaux d’infiltration est observée à Soloco durant les épisodes de crue. A l’échelle du bassin du Haut Marañon, les massifs calcaires Nord Andins exportent chaque année environ 7462.10^3 tonnes d’éléments dissous, ce qui représente 70% des flux exportés par les fleuves Haut Marañon et Huallaga. Le taux d’ablation a été estimé à environ 70 mm.Kyr^{-1} pour le karst de Soloco, et 53 mm.Kyr^{-1} pour le karst de Palestina. Ces valeurs confirment une tendance globale selon laquelle l’écoulement annuel est le principal facteur contrôlant l’érosion karstique.

INTRODUCTION

Karst aquifers in tropical zones remain few studied today, mainly because of logistical difficulties inherent to the sites (abundant vegetation, absence of roads to access to the sites). Most of the existent studies were conducted in Jamaica , Belize (Miller, 1983) and in Asia (see for example Crowther, 1989; Han and Liu, 2004; Han et al., 2010; Li et al., 2010; Liu et al., 2013; Yan et al., 2012) almost to study the ablation of the karst.

In South America, various studies of the hydrology and hydrochemistry of the karsts were realized, in particular in Brazil, Bolivia and Mexico (see for example Auler, 1994, Eraso et al., 2001, Gondwe et al., 2010, Steinich & Marín, 1997). Some of these studies are also about the relationship between the climate and the hydrology of the karst (F.W. Cruz Jr. et al., 2005), the paleoflow analysis (Auler, 1998). Furthermore, during these last years, several studies on the current flow conditions and paleoclimate were conducted in these regions, thanks to the growing knowledge in the use of trace elements (see for example Karmann et al., 2007; Cruz et al., 2009; Winter et al., 2011)

In the Northwest of Peru studies of karsts begin to be realized, especially thanks to the speleological expeditions led by the GSBM (Groupe Spéléo Bagnols Marcoule), the GBPE (Grupo Bambuí de Pesquisas Espeleológicas) and the ECA (Espeleo Club Andino) in this region (CESPE, GBPE, GSBM, 2004; ECA, CESPE, GSBM, 2006; ECA, GSBM, 2008), and to the HYBAM (HydroGéodynamique du Bassin Amazonien) and Paleotracés projects led by the IRD (French Institute of Research for the Development). These reports present mainly the caves network descriptions and short studies on the hydrology and climate of this region (Guyot et Lavado, 2004) and the hydrolocal regime of the Soloco resurgence (Guyot, 2006).

On a global scale, the weathering of carbonates is the predominant phenomenon in the release of dissolved material in rivers (Meybeck, 2003). Andean sub-basins (Marañon and Ucayali) of the Amazon basin highly control the geochemistry of the Amazon river (Moquet et al., 2011). The alteration of the large outcrops of the Upper Triassic - Lower Jurassic limestones in these sub-basins can respectively contribute to 35-50%, 40% and 58% of the production of Calcium, Magnesium and Carbonates transported by the Amazon, in an area corresponding to less than 5% of the basin. Otherwise, Marañon and Ucayali basins contribute respectively to 8% and 6% of the total discharge of the Amazon river (Moquet, 2011).

Moreover, the abundant rainfall in these regions and the large recharge zone of these karst aquifers provide them a large supply of groundwater (Peña, 2012).

Thus, monitoring the hydrology and chemistry of the karst basins of the Amazon can allow to better understanding the dynamics of the release of dissolved material in this medium and its contribution to the flux exported by the Amazon River.

In the framework of the projects HYBAM and Paleotracas, a study of the karstic resurgences of Soloco (Chachapoyas, Amazonas, Peru) and Palestina (Rioja, San Martin, Peru) which drained the High Marañon basin has been led. These two resurgences belong to two distinct zones of the basin, as Soloco is located in the Cordillera Oriental (at 2630 m a.s.l.) while Palestina is situated in the Amazonian Piedmont zone (870 m a.s.l.) (Fig. 1).

Based on the study of hydrological and chemistry data running from 2006 to 2012 for Soloco, and from 2011 to 2012 for Palestina, the first part of the work conducted during this internship aims to give an overview of the hydrogeological behavior of these two resurgences through the comparison of their hydrological and hydrogeochemical regimes. The second part aims to study the contribution, in terms of discharge and flux of dissolved solids, of these two resurgences, and at a larger scale, of the North Andean calcareous massifs to the High Marañon and the Huallaga rivers. Finally, the third part aims to calculate the karstic ablation rate of the catchments studied.

Chapter 1. The karsts of the massif of Soloco and of the massif of the Alto Mayo: presentation of the two resurgences studied

1. GEOGRAPHIC CONTEXT

The Amazon river ($5960 \cdot 10^3 \text{ km}^2$, $206\,000 \text{ m}^3/\text{s}$) is largest river of the world (Callède et al., 2010) and 10% of his drainage basin is located in the Andes. In Peru, the mean Andean tributaries of the Amazon river are: 1. the Marañon river ($361 \cdot 10^3 \text{ km}^2$, $16200 \text{ m}^3/\text{s}$) that drains the Andean rivers from Colombia to North Peru, and the Ucayali river ($347 \cdot 10^3 \text{ km}^2$, $11400 \text{ m}^3/\text{s}$) that drains Central and Southern part of the Peruvian Andes (Guyot et al., 2007; Armijos et al., 2013).

The two studied areas are located in the North Andes of Peru, Soloco river as a part of the Utcubamba river basin (a tributary of the high Marañon river), and Jordan river (issued from Palestina Cave) as a part of the Mayo river basin (a tributary of the Hualaga river, which join downstream in the floodplain the Marañon river).

The resurgence of Soloco is situated in the karstic massif of Soloco (Cordillera Oriental) at an altitude of 2630 m a.s.l., at about 20 kilometers at the SW of the town of Chachapoyas (Province of Chachapoyas, extreme south of the region of Amazonas, North West of Peru). This massif stretches in about 50 km^2 , between 6.28°S and 6.36°S of latitude and 77.72°W and 77.81°W of longitude. Its altitudes ranging from 2000 m to 3348 m (Fig. 1 and Table 1).

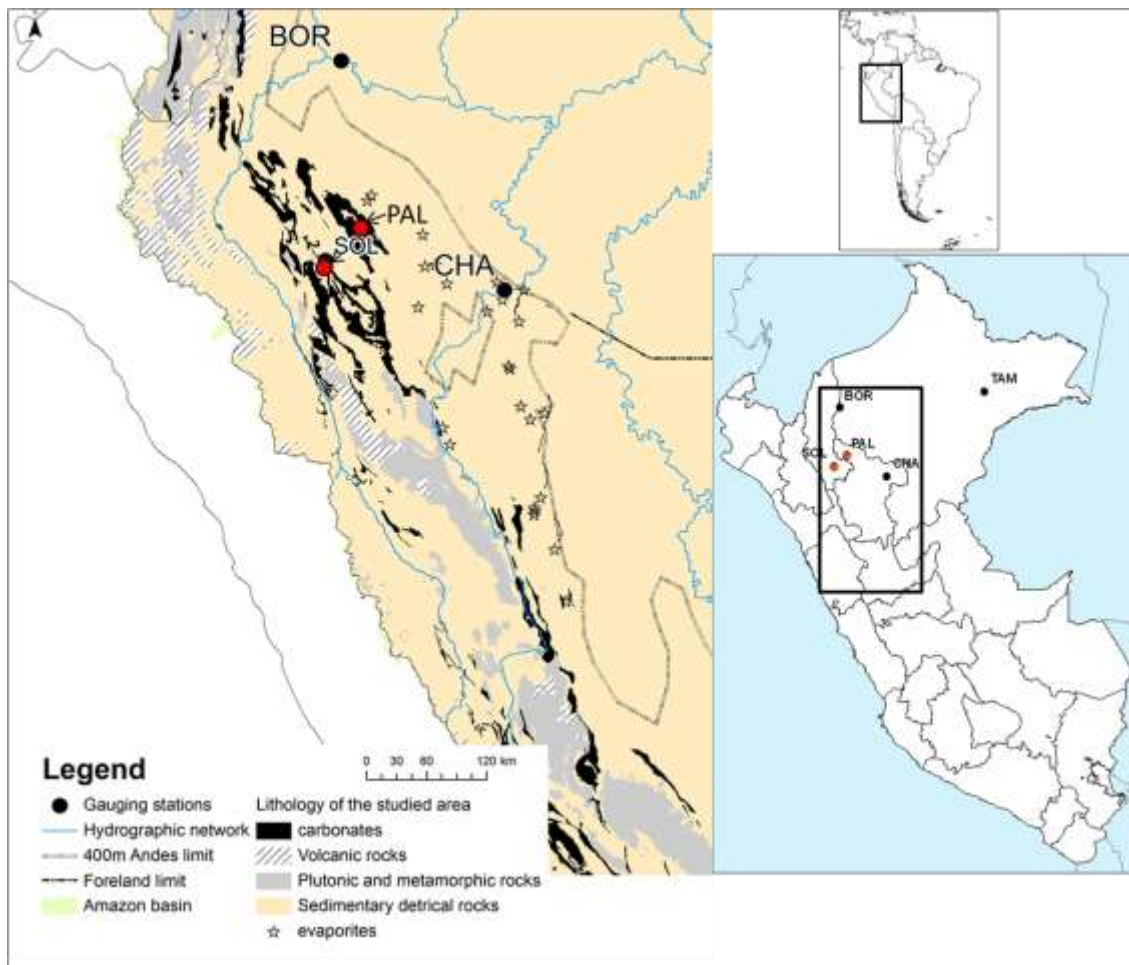


Figure 1: Localization of the resurgences of Soloco (SOL) and Palestina (PAL) (source: Moquet, 2011, modified)

The resurgence of Palestina is located in the massif of the Alto Mayo, in the Amazonian piedmont, at an altitude of 870 m a.s.l. (Province of Rioja, extreme North of the San Martín region, North West of Peru) which is situated between a latitude of 5.67°S and 6.22°S and cover an area of about 300 km² (Fig. 1 and Table 1). Its altitude range from 850 m at the foot hill and 2400 m at the level of the highest summits.

This massif forms a distinct unit and belongs to the sub-andine zone. It is oriented NNE-SSW and is limited at the NE for the depression of Rioja, and at the SW by the catchment of the Río Chiriaco (Morales-Bermúdez, 2004 in CESPE, GBPE, GSBM,, 2004).

Table 1: resurgences studied in the framework of this internship. Lat.: latitude; Long.: longitude; Alt.: altitude; A_{BY} : Area of the catchment; Q_m : mean discharge; Q_{max} : maximum discharge; Q_{min} : minimum discharge..

Name	Lat.	Long.	Alt. (m a.s.l)	A_{BY} (km^2)	Period	Q_m ($m^3 \cdot s^{-1}$)	Q_{max} ($m^3 \cdot s^{-1}$)	Q_{min} ($m^3 \cdot s^{-1}$)
Palestina	5.9258°S	77.3507°W	870	15	2011-2012	0.50	0.53	0.47
Soloco	6.2809°S	77.7488°W	2630	26	2006-2012	1.07	1.20	0.95

1.1. Climatic context

The High Marañon basin is submitted to an intermediate regime between Southern tropics and the equator which features a very rainy period from January to April and a dryer period from May to September (Espinoza Villar et al., 2009). The mean annual rainfall is about $1404 \text{ mm} \cdot \text{yr}^{-1}$ at Rioja (1963-2012 period) (Fig. 2), and $824 \text{ mm} \cdot \text{yr}^{-1}$ at Chachapoyas (1963-2012 period) (source: Servicio Nacional de Meteorología e Hidrología (SENAMHI)).

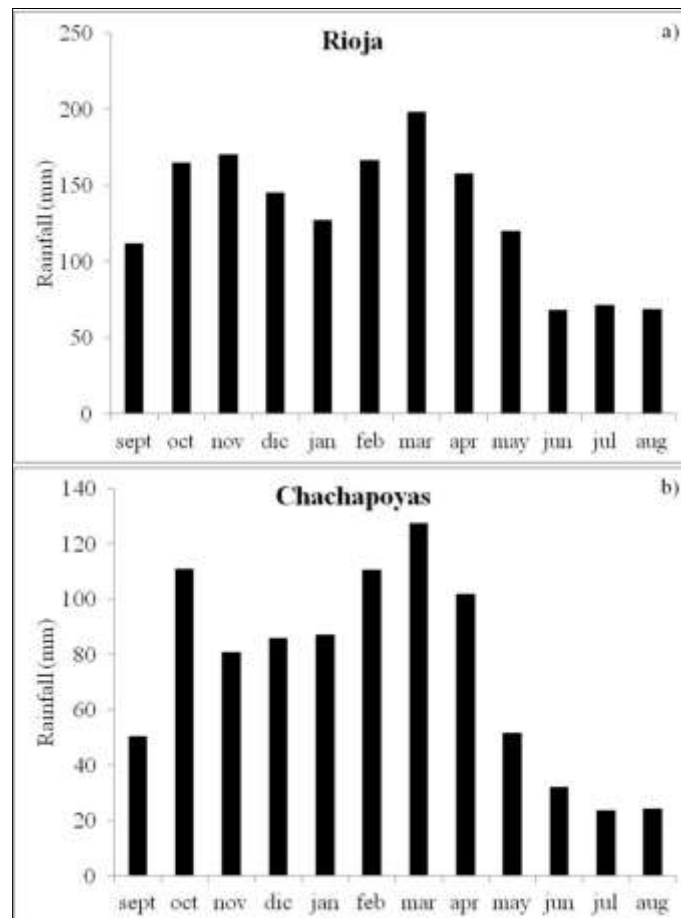


Figure 2: Monthly rainfall: a) at the station of Rioja (X:-6.033 S, Y:-77.167 W, Z: 848 m a.s.l.); b) at the station of Chachapoyas (X:-6.205 S, Y:-77.867 W, Z: 2334 m a.s.l.)

The abundant rainfall in these regions (almost in Palestina) is related to the moist warm air and to the release of high quantity of water vapor over the first eastern slopes of the Andes (Espinoza Villar et al., 2009).

The rainfall is measured with a pluviometer Davis (registering time step: 1 hour) since the 16/05/2011 at Soloco and since the 01/06/2012 at Palestina.

At Palestina, the pluviometer is located at about 500 m of the resurgence, at the same altitude. For the resurgence of Soloco, the pluviometer is installed in the village of Soloco, at about 2.7 km downstream the resurgence. Thus, the rainfall measured by the pluviometer is not totally representative of the rainfall at the level of the resurgence.

The available data run from the 01/06/2012 to the 07/02/2013 at Palestina. At Soloco, they run from the 16/05/2011 to the 20/01/2012 and from the 27/05/2012 to the 07/02/2013.

Consequently, we couldn't use the data of the pluviometers to estimate the annual rainfall at both resurgences. We will use the pluviometric gradients to have an estimation of the annual rainfall.

The pluviometric gradient is about +185 mm/yr/100 m for Chachapoyas, and -21 mm/yr/100 m for Rioja (Guyot et Lavado, 2004) (Fig. 3a). The temperature gradient for the two regions is 0.6°C/100 m (Fig. 3b).

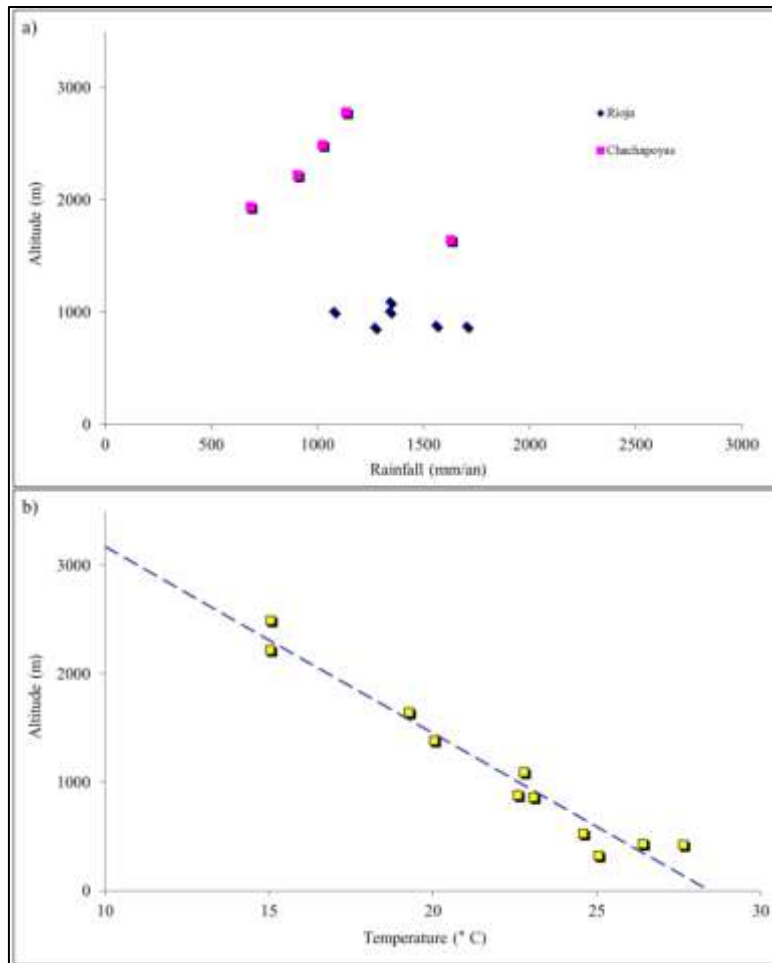


Figure 3: a) Altitudinal pluviometric gradient; b) Altitudinal temperature gradient for the areas of Rioja and Chachapoyas (source: Guyot, 2004)

According to the pluviometric gradients, the mean annual rainfall would be about 1372 mm.yr^{-1} at the level of the resurgence of Soloco, and 1400 mm.yr^{-1} at the resurgence of Palestina.

1.2. The karstic systems

1.2.1. Palestina

1.2.1.1. Geology of the catchment

The karst of Palestina is situated in the massif of the Alto Mayo (Amazonian piedmont) which is structurally defined by the anticlinal of the Cerro Blanco (Fig. 4). The Pucará group forms the sides of this anticlinal. This group is composed: at its base by the gray limestone with chert nodules and beds of yellowish gray micritic limestone in layers of 2 to 3 meters of the Chambará formation; in the middle by the limestones and

argillaceous silt of the Aramachay formation; and at the top by the stratified thin black limestones with calcite veinlets of the Condorsinga formation (Fig. 4).

The sides of this fold are slightly tightened and present dips of 30 to 45°. The argillaceous sandstones and the conglomerates of the Mitu group form the core of the fold (source: Instituto Geológico, Minero y Metalúrgico (INGEMMET)). The karst is developed in the Chambará formation, and the resurgence of Palestina is situated on the inverse fault of Santa Cruz which contacts the Aramachay and the Condorsinga formations (Fig. 4).

The catchment is limited at the north-west by the crest of the Cerro Condor, at the west by the contact between the Mitu group and the Chambará formation and has an area of about 15 km². It culminates at 2037 m a.s.l. and the resurgence of Palestina (870 m a.s.l.) is the lowest point of the catchment (Fig. 4). The average slope of the catchment is 25.4%.

The limits of the catchment are still imprecise for the moment. More advanced investigations, especially the realization of dye tracings, would allow to better define the geometry of the catchment.

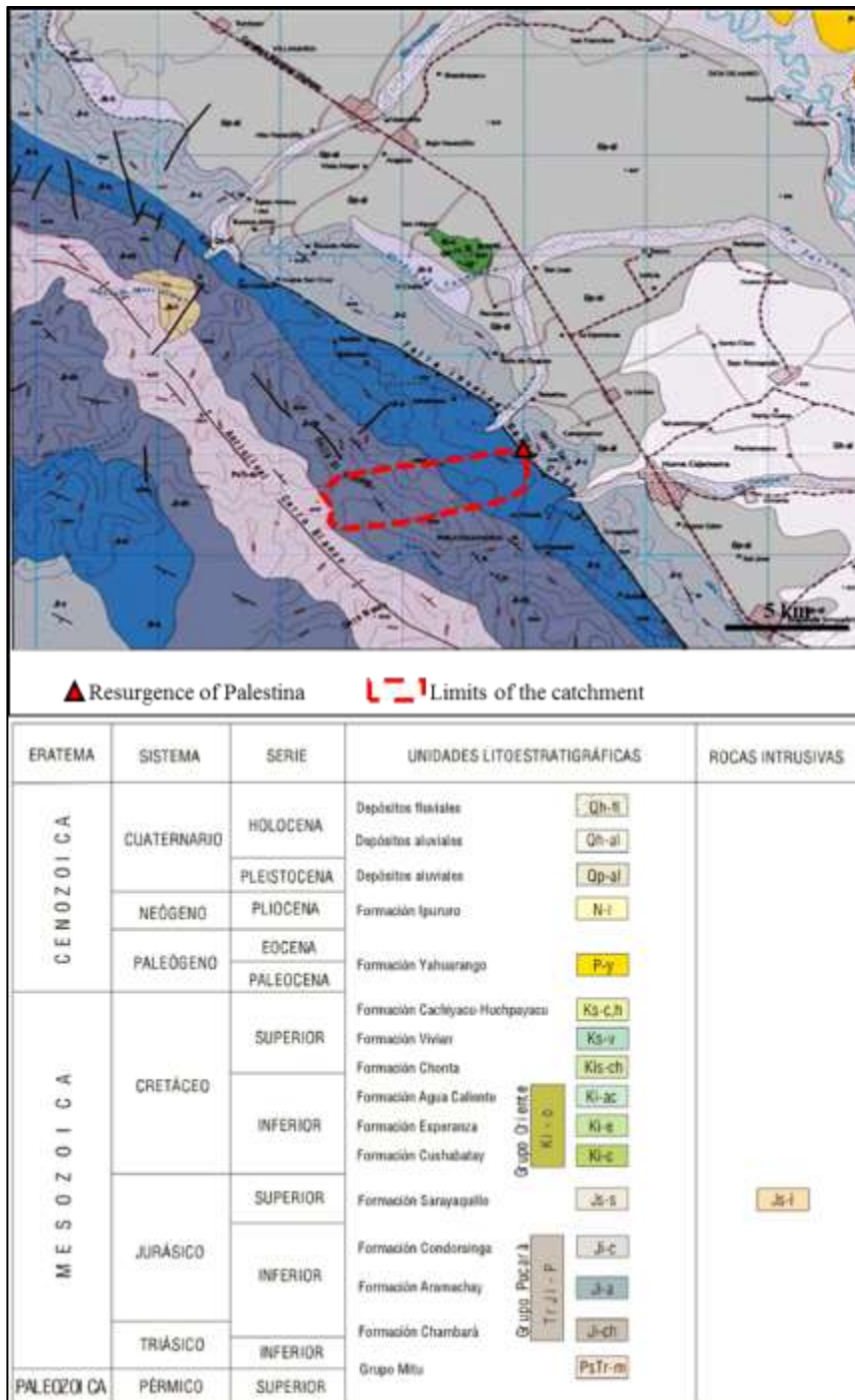


Figure 4: Theoretical catchment of the resurgence of Palestina

1.2.1.2. Karstic morphology of the Alto Mayo

The massif presents a morphology of exo-karst, with numerous canyons, karstic cliffs, dolines and lapiaz (Morales-Bermúdez, 2004 in (CESPE, GBPE, GSBM., 2004). This morphology is the result of hexogen erosive processes as the intensity of the runoff (Huaman, 2004 in (CESPE, GBPE, GSBM., 2004).

1.2.2. Soloco

1.2.2.1. Geology of the catchment

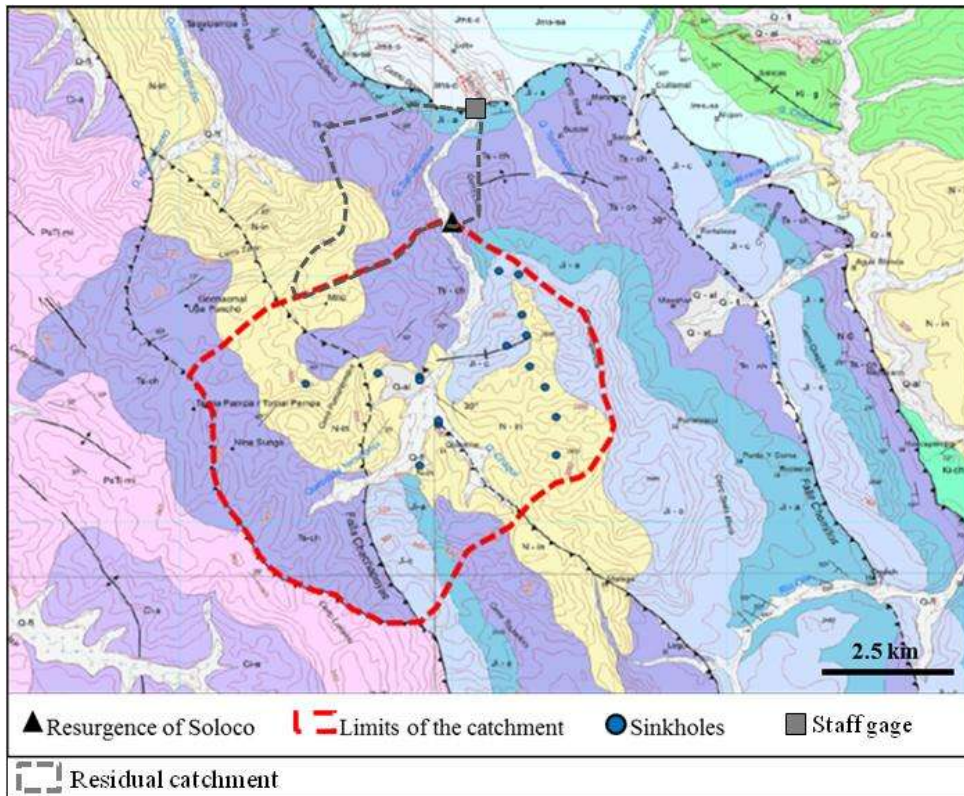
The karst of Soloco is developed in the Chambará formation (Fig. 5) which is composed at its base by recrystallized limestones with abundant chert nodules and with some intercalations of clays. The top of the formation is composed by *mudstone* and *packstone* limestones alternated with levels of dolomite, shales and sporadic volcanic ashes.

Around a third of the catchment is covered by the tuffaceous sandstones and conglomerates of the Inguilpata formation (Neogene) (source: INGEMMET)

Numerous inverse faults oriented NNW-SSE divide the massif in several units. The major part of the karstic network is developed on the east side of an anticline, at the east of the Triunfo faults system (Fig. 5)

The catchment, limited at the south-west by the Chachapoyas fault, at the south-east by the crest of the Cerro Tragadero and at the east by the crest of the Cerro Chupunche, has an area of about 26 km² and culminates at 3348 m a.s.l. The resurgence of Soloco, situated at 2630 m a.s.l., is the lowest point of the catchment (Fig. 5). The average slope of the catchment is 17.9%.

The distance between the resurgence and the staff gage (about 2.5 km) (see Chapter 2, §1.1.2.1.) leads to the creation of a residual catchment of about 5 km² (Fig. 5).



ERA	SISTEMA	SERIE	UNIDADES LITOESTRATIGRAFICAS
CENOZOICO	CUATERNARIO	Holoceno	<p>Depósitos coluviales Clastos de diversos tamaños angulosos-subangulosos, englobados en una matriz limo-arenosa formados al pie de las laderas. Gran parte de estos depósitos sirven como tierras de cultivo.</p> <p>Depósito fluvial Gravas con clastos redondeados, envueltos en una matriz arenosa con pequeños lentes de arena, que se encuentran a lo largo del río formando terrazas.</p> <p>Depósito aluvial Acumulaciones de gravas, arenas, limos con clastos redondeados-subredondeados de composición polimictica, ubicados en las quebradas y con cierta clasificación.</p> <p>Dis. Erosional</p>
		NEÓGENO	Plioceno
MESOZOICO	CRETÁCICO	Superior	<p>Formaciones Chulec Calizas de color beige con estratos delgados e intercalación de margas.</p> <p>Grupo Boylariscuzza Areniscas cuarzosas de color blanco, con algunas intercalaciones de lutitas, y limolitas de coloraciones gris verdosas.</p> <p>Dis. Erosional</p>
		Inferior	<p>Formación Corontachaca Brechas sedimentarias conformadas por fragmentos angulosos y subredondeados de caliza, en una matriz fuertemente cementada de material calcáreo. Intercalaciones de conglomerados y areniscas rojas.</p>
	JURÁSICO	Superior	<p>Formación Condorsinga Calizas de color gris a beige en estratos delgados entre 10 a 40 cm. Superficies de estratificación onduladas. Por interperimio presenta coloraciones blanquecinas.</p>
		Inferior	<p>Formación Aramachay Calizas arcillosas gris oscuro a negro, bituminosa de colores gris y negro bien estratificadas y laminadas, intercaladas con arcillas calcáreas y lutitas bituminosas con amonites.</p> <p>Formación Chambará Calizas recristalizadas grises, masivas, con coloraciones superficiales beige a marrón claro, plegadas, con folias y con algunos niveles de calizas dotmíticas.</p> <p>Dis. Erosional</p>
	TRIÁSICO	Superior	<p>Formación Yahuarango Areniscas feldespáticas con intercalaciones de lutitas grises y rojas.</p>
	PALEOZOICO	PÉRMICO	Superior
CARBONIFERO		Inferior	<p>Formación Chonta Lutitas negras con intercalaciones de calizas y areniscas grises en la base.</p> <p>Grupo Oriente Areniscas cuarzosas blancas, con laminación oblicua y horizontal con algunas intercalaciones de lutitas negras.</p> <p>Formación Sarayakuillo Intercalación de areniscas y lutitas rojas con algún nivel o brecha con clastos de calizas y con algunos niveles de areniscas cuarzosas de coloraciones amarillentas.</p>

Figure 5: Theoretical catchment of the resurgence of Soloco

1.2.2.2. Karstic morphology of the massif of Soloco

The presence of numerous mega-sinkholes, with a depth almost higher than 100 m, gives to this massif a morphology of “sinkholes joined karst” typical of the tropical karsts (Couturaud, 2006 in (CESPE, ECA, GSBM,, 2006). The summits of the numerous mounds present in the massif are constituted by sharp peaks (pinnacles, limestone needles) which attest of an important erosion (Bigot, 2008 in (ECA, GSBM,, 2008).

1.3. A first overview of the hydrogeology of the two resurgences

1.3.1. Resurgence of Palestina

The first data collected (19/05/2011 to 28/09/2012) showed that the waters of the resurgence are calcium bicarbonate type, with a conductivity of about $220 \mu\text{S}\cdot\text{cm}^{-1}$ and a temperature of 20°C . The value of EC is of the same order of magnitude than those measured at the resurgences of Tigre Perdido and Shatuca, located nearby, by Moquet et al. (2009). The mean discharge is about $0.43 \text{ m}^3\cdot\text{s}^{-1}$.

1.3.2. Resurgence of Soloco

The first measures realized in 2004 on the Rio Soloco have allowed estimating discharges between 0.6 and $1.8 \text{ m}^3\cdot\text{s}^{-1}$ (Couturaud, 2006 in CESPE, ECA, GSBM,, 2006). A measure realized in February 2007 confirms these values, estimating a discharge of $1.18 \text{ m}^3\cdot\text{s}^{-1}$ and a conductivity of $213 \mu\text{S}\cdot\text{cm}^{-1}$ (Guyot, 2006 in CESPE, ECA, GSBM,, 2006)..

The waters of the resurgence are little mineralized (54 to $174 \text{ mg}\cdot\text{L}^{-1}$), with a temperature of about 12.8°C , and are calcium bicarbonate type. Their chemical composition is very similar to that of the runoff waters (Guyot, 2006 in CESPE, ECA, GSBM,, 2006).

Chapter 2. The resurgences of Soloco and Palestina: acquisition and treatment of data

1. ACQUISITION OF HYDROLOGICAL AND PHYSICAL CHEMISTRY PARAMETERS

A high frequency monitoring of the hydrological and physical chemistry parameters is realized at each resurgence. The monitored parameters are the following: the water level outside the cave (staff gage), and inside the cave (CTD-Diver); the electrical conductivity (EC) and the temperature of water inside the cave (CTD-Diver); the atmospheric pressure and the temperature of air inside the cave (Baro-Diver). The Table 2 resumes the equipment used.

Table 2: Name of the resurgence, with the equipment in place, parameters measured, the monitoring time step, the accuracy of each equipment, and the available data.

Resurgence	Equipment	Measure (units)	Monitoring time step	Accuracy	Available data
Soloco	Staff gage	Water level (cm)	2 readings/day (08/2005-12/2008)	± 3 cm	01/08/2005-30/12/2008
			1 reading/day (8:00 a.m.) (09/2010 to present)		01/09/2010-30/09/2012
	CTD-Diver	Water level (cm H ₂ O)	15 min	± 0.2 %	27/05/2012-25/09/2012
		EC at 25°C (µS.cm ⁻¹)		± 1 %	
Baro-Diver	Temperature of water (°C)	15 min	± 0.2 °C	27/05/2012-06/02/2013	
	Atmospheric pressure (cm H ₂ O)		± 2 cm H ₂ O		
Palestina	Staff gage	Water level (cm)	2 readings/day (15/09/2011-present)	± 1 cm	15/09/2011-21/01/2012
					01/04/2012-06/04/2012
	CTD-Diver	Water level (cm H ₂ O)	15 min	± 0.2 %	19/05/2011-07/02/2013
		EC at 25°C (µS.cm ⁻¹)		± 1 %	
Baro-Diver	Temperature of water (°C)	15 min	± 0.2 °C	19/05/2011-28/09/2012	
	Atmospheric pressure (cm H ₂ O)		± 2 cm H ₂ O		
		Temperature of the cave (°C)		± 0,2 °C	

The water levels outside the caves are measured by an observer working with HYBAM and living near to the resurgence.

The gauging of the resurgences is performed during the field missions with an OTT C31 propeller-type current meter.

1.1. Treatment of data

1.1.1. Recuperation of data

Hydrological data (HYBAM observer water levels and CTD water levels), physical chemistry data (conductivity and temperature of water) and chemistry data (samples of water) for the two resurgences were recuperated during the first field campaign HYBAM-Paleotracés, in February 2013 (04/02/13 to 22/02/13).

At Soloco, the unloading of the data of the Baro-Diver was realized without inconvenient, registering data from the 29/09/2012 since the 06/02/2013. The data of the CTD-Diver weren't unloaded because the captor couldn't be removed. Consequently, they couldn't have been treated in the framework of this internship.

The unloading of the CTD-Diver of Palestina was realized normally. The data registered run from the 19/05/2011 to the 07/02/2013. However, the Baro-Diver was out of order, so the data couldn't be recovered.

1.1.2. Treatment of data

Hydrological and chemistry data were treated using the Hydraccess software developed in the framework of the HYBAM project (Vauchel, 2005) (free download at <http://www.ore-hybam.org/index.php/eng/Software/Hydraccess>). The procedure has consisted in create a captor assembling all the available data for each parameter studied.

The discharges of both resurgences was calculated using the water levels and the calibration curve. Data of concentrations of each major element were used to calculate the fluxes of elements exported by both resurgences (see §4. for more details).

1.1.2.1. Resurgence of Soloco

The monitoring of the resurgence has begun in August 2005. The station was stopped between December 2008 and September 2010 before to start again. The water levels on the staff gage were read twice a day (8:00 am and 18:00 pm) before December 2008 and only once a day since September 2010 (08:00 am) (see Table 2). Consequently the available data of water levels run from the 01/08/2005 to the 30/12/2008 and from the 01/09/2010 to the 30/09/2012 (Table 2 and Fig. 6).

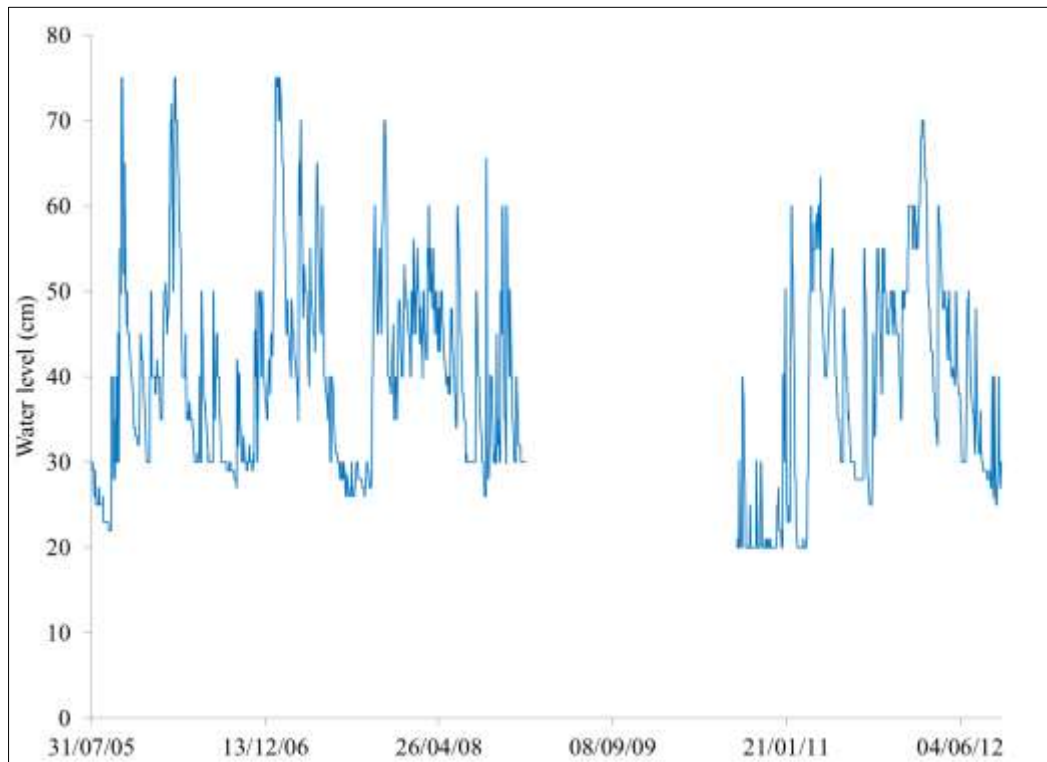


Figure 6: Water levels of the Rio Soloco (Resurgence of Soloco)

In September 2011, a first CTD-Diver was installed downstream the resurgence at about 100 m. This CTD was snatch during a flood and has never been found.

In May 2012, a second CTD-Diver was installed in a well inside the cave leading to the underground river. The Baro-Diver was installed in the same time.

The staff gage is located in the village of Soloco, very downstream of the resurgence (at about 2.5 km), in a narrowing of the Rio Soloco. Consequently, a strong softening of the hydraulic charge is observed at the level of the staff gage (Fig. 7a), what is confirmed by the relation $H_{Obs} = f(H_{CTD})$ (with H_{Obs} : staff gage water level and H_{CTD} : CTD water level) which is not linear (Fig. 7b).

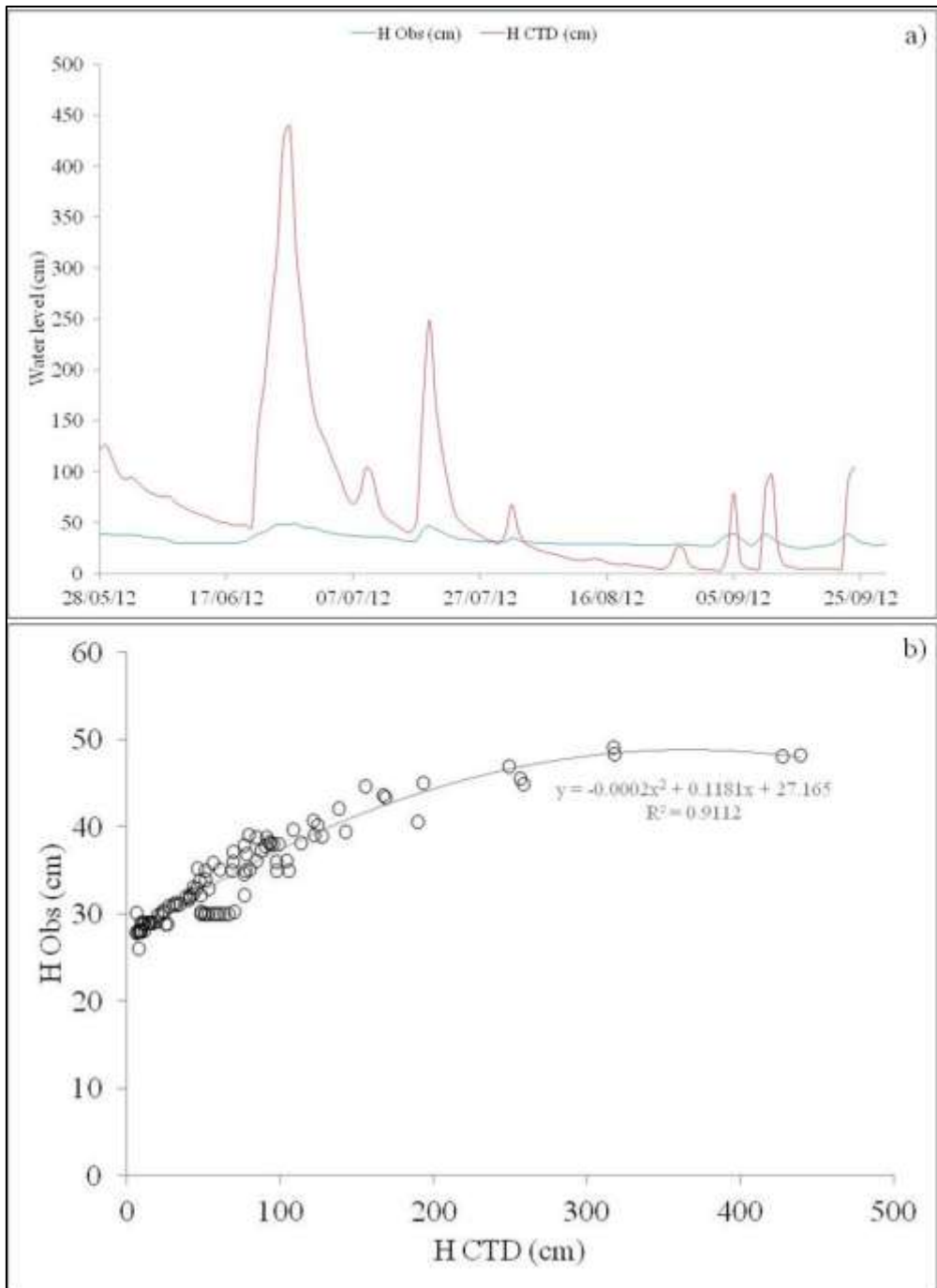


Figure 7: a) staff gage and CTD water levels registered at the resurgence of Soloco; b) relation between the discharge and the CTD water levels of the resurgence of Soloco.

During floods, the strength of the flow can displace rocks and discalibrate the relation Water level-Discharge. Moreover, the waves generated during the flood don't allow reading with precision the level on the staff gage: the error of reading could be about more or less 3 cm (Table 3), which represents 10% of the total amplitude of the level of the river. Consequently, it was decided to establish a calibration curve with a superior and inferior limit (Fig. 8).

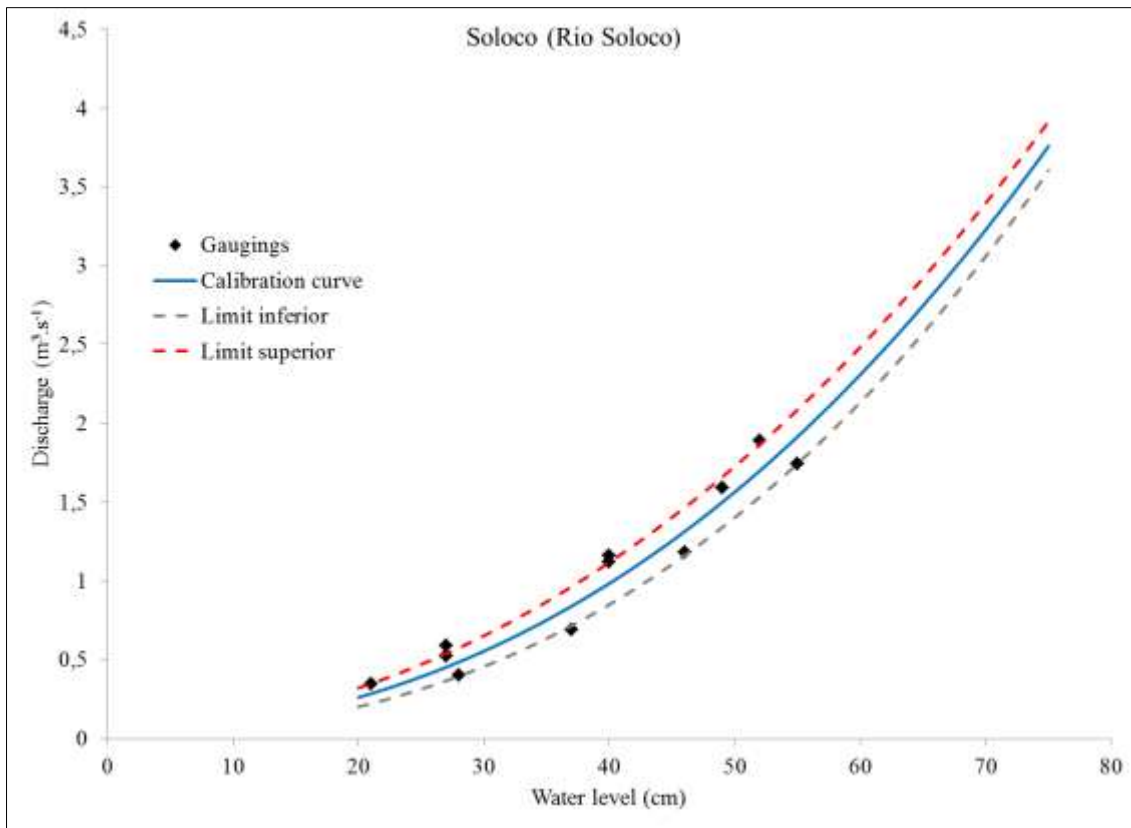


Figure 8: Calibration curve of the resurgence of Soloco (Rio Soloco)

1.1.2.2. Resurgence of Palestina

At Palestina, a first gaging was realized in May 2011, without reference to a staff gage but after the installation of a first CTD-Diver (CTD1) (Table 3).

Table 3: Chronology of the functioning of the equipments of the resurgence of Palestina.

19/05/11	31/08/11	15/09/11	21/01/12	01/04/12	02/04/12	16/04/12	24/05/12	02/06/12	28/09/12	07/02/13
No staff gage			CTD 1				CTD 2			
No staff gage			R1				No staff gage			
Baro-Diver operational			Baro-Diver out of order				Baro-Diver operational		Baro-Diver out of order	

In September 2011, a staff gage was installed (R1), with a reference boundary stone. This reference boundary stone was removed during the built of a house. In April 2012, woodcutters used the Rio to transport wood. The trunks snatched the staff gage. During the field campaign of May 2012, a new staff gage (R2) and CTD-Diver (CTD2) were installed (Table 3).

Consequently, it doesn't exist a common period of observation for R1 and R2 (Fig. 9), neither for CTD1 and R2 or CTD2 and R1. So it will be necessary to use the gagings to bring together the series of water levels measured on R1 and R2.

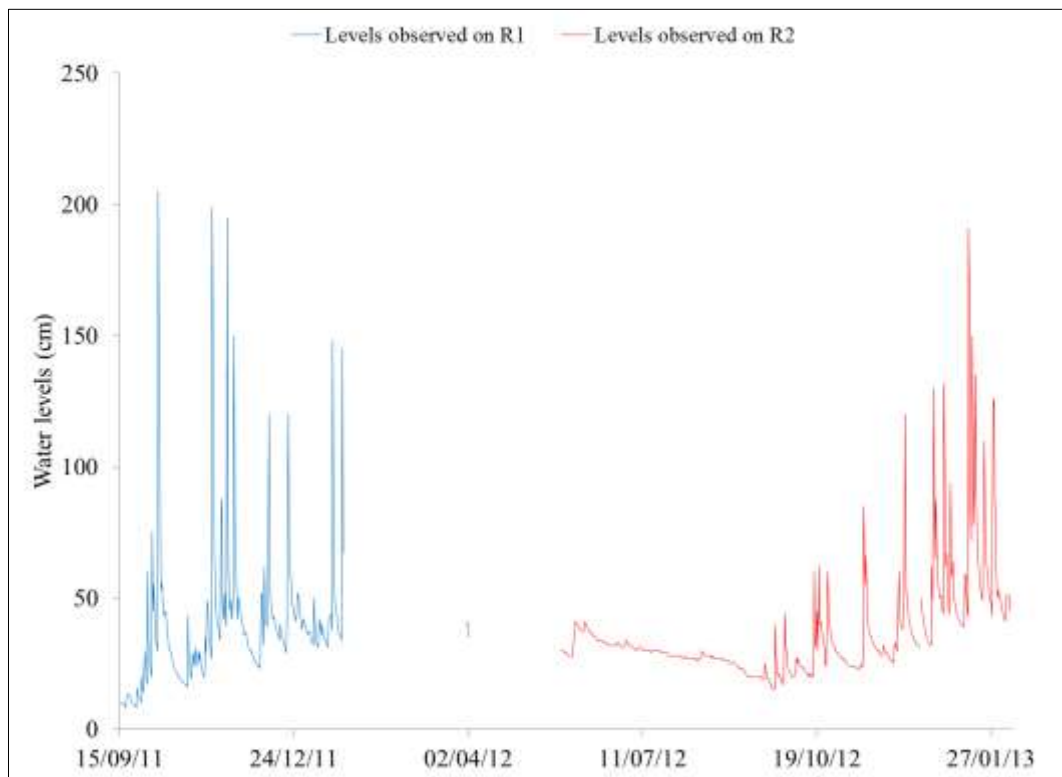


Figure 9: Levels observed on R1 and R2 at Palestina

A first calibration curve was traced with the three gagings realized before May 2011 (Fig. 10). The last two gagings are situated below at the right, at 9 cm, of the calibration curve. So it has to add 9 cm to the levels read on R1 to obtain a unique serie of levels on the referential of R2.

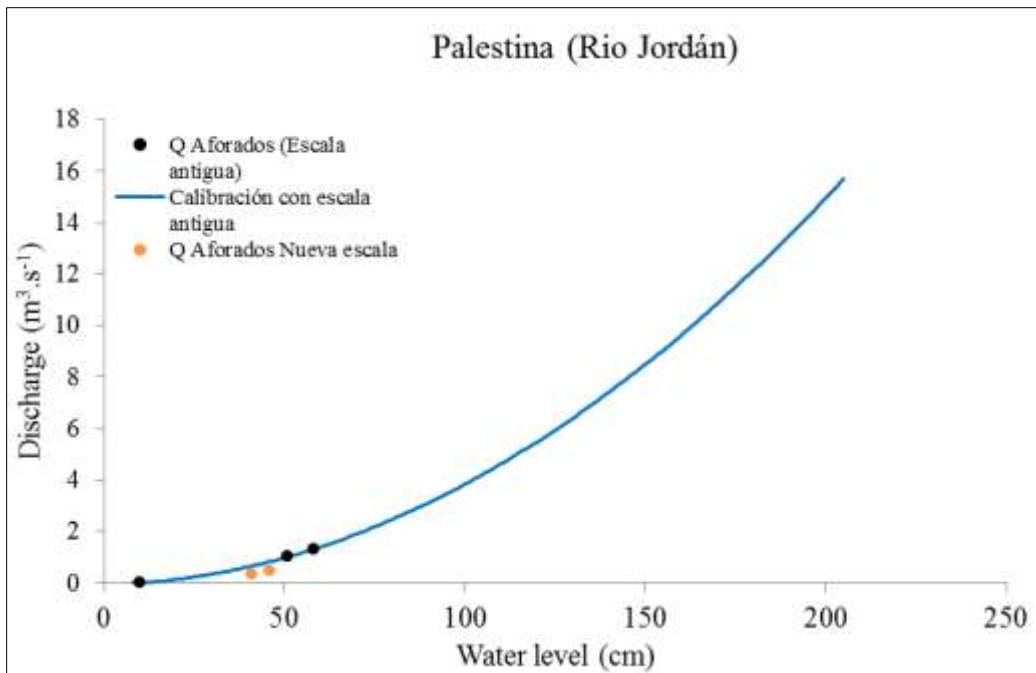


Figure 10: First calibration curve of the resurgence of Palestina (Río Jordán)

Then, it has to find a relation between the series of water levels measured by the observer and those of the CTD1 and the CTD2.

For the CTD2 and R2, the following relation was found (Fig. 11):

$$\mathbf{H_{R2} = H_{CTD2} - 4cm}$$

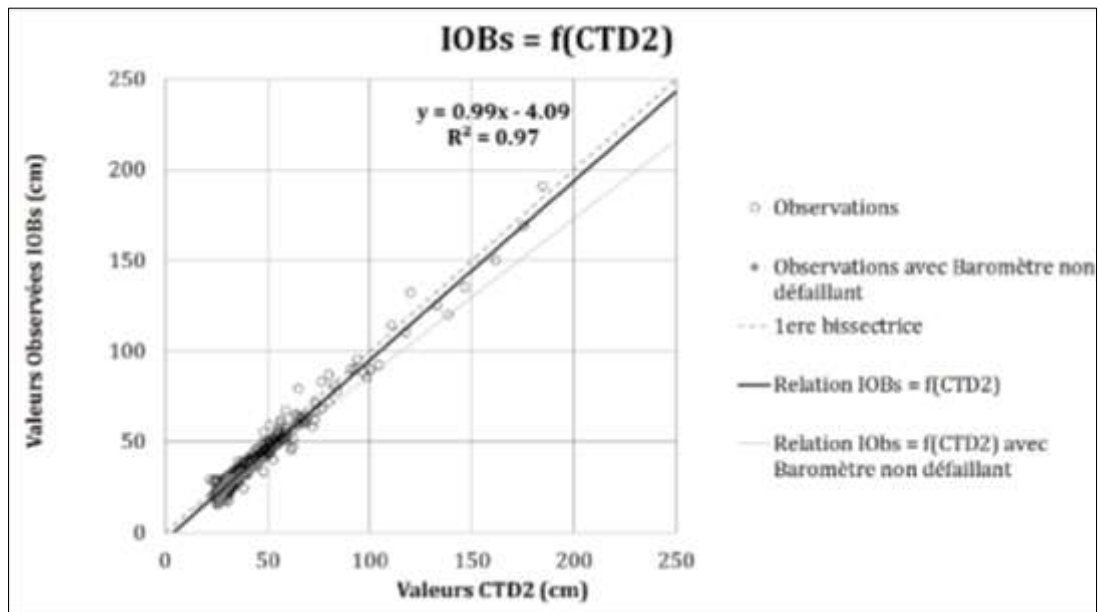


Figure 11: Relation between the levels measured on R2 and the levels registered by the CTD2 at Palestina

We search then a relation between the levels measured by the observer and the levels measured by the CTD1 (Fig. 12). We can see that three periods can be identified for the CTD1.

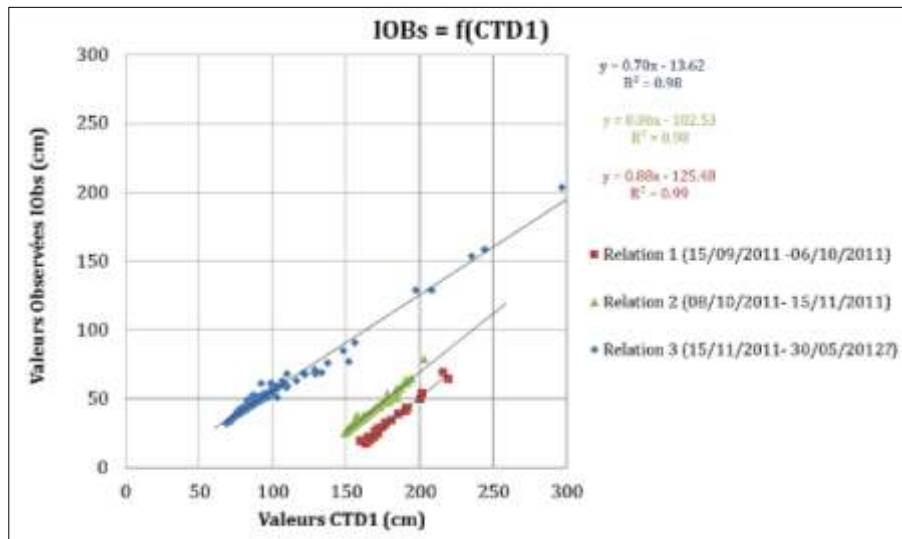


Figure 12: Relation between the levels measured on R1 and the levels registered by the CTD1 at Palestina

The following serie of water levels expressed in the referential of R2 is obtained (Fig. 13):

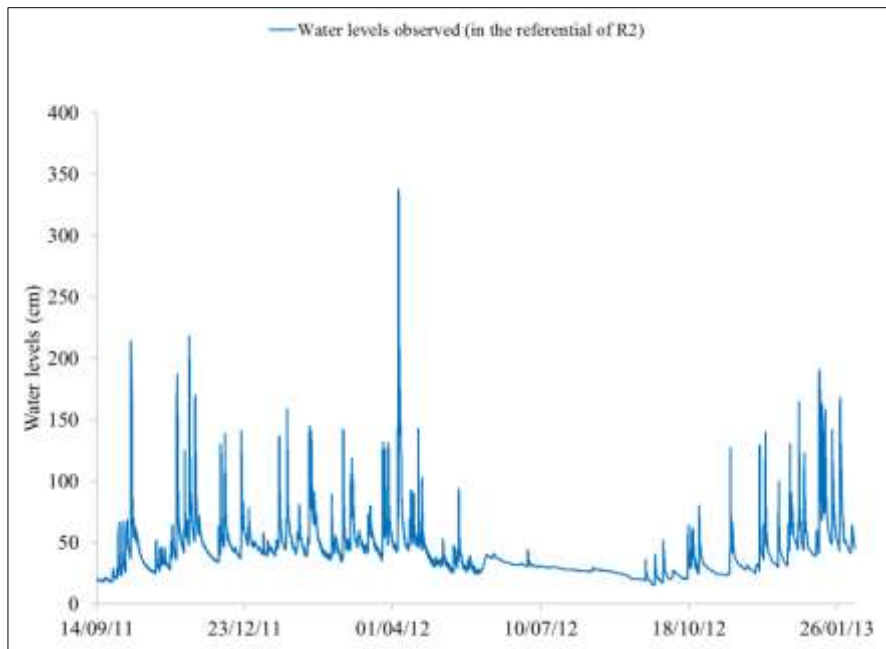


Figure 13: Water levels expressed in the referential of R2 at Palestina

It stays now to express the levels registered by the CTD1 of the period running from May 2011 to September 2011 where no staff gage was installed (see Table 3). The first reading on the staff gage R1 (the 15/09/2011) allows to readjusting the levels registered by the CTD1. It is seen from Figure 14 that it has to add 4 cm to the levels registered by the CTD1 between May 2011 and September 2011.

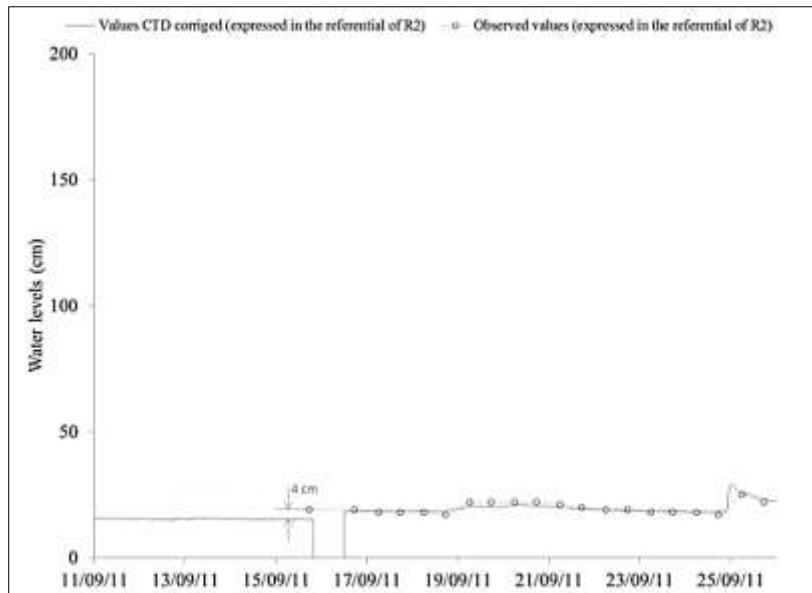


Figure 14: Readjustment of the levels registered by the CTD 1 before the 15/09/2011

We finally obtain the following serie of water levels for the resurgence of Palestina (Fig. 15):

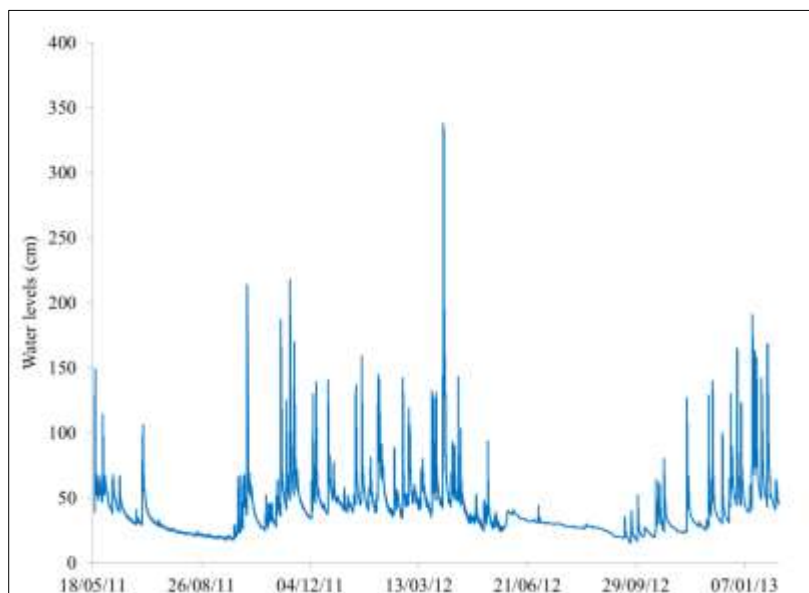


Figure 15: New serie of water levels in the referential of R2 at Palestina

In order to verify the results obtained, we have used the first gauging realized in May 2011. The water level corresponding at the hour of the gauging is 64 cm. We can see that the point is aligned on the calibration curve (see Fig.16).

We can now trace a new calibration curve for the resurgence of Palestina. The water levels of the stream gagings were replaced in the referential of R2 adding 9 cm (Table 4).

Table 4: Stream gagings realized at the resurgence of Palestina. H (R1): water levels expressed in the referential of R1; H (R2): water levels expressed in the referential of R2.

Date	H (R1) (cm)	H (R2) (cm)	Q (m ³ .s ⁻¹)
21/05/2011 13:30	-	64	1.073
16/09/2011 00:00	19	28	0.00
21/01/2012 16:00	67	76	1.321
22/01/2012 10:00	58	67	1.025
01/06/2012 10:00	-	41	0.354
13/02/2013 10:00	-	46	0.5
25/06/2013 12:15	-	31	0.00

The little number of stream gagings, and the weak discharges gauged don't allowed tracing a precise calibration curve. Consequently, it is necessary to confine the values of discharge proposing a superior and inferior limit (see Fig. 16).

These limits were proposed adjusting the value H_0 for which the discharge is null. Due to the absence of high discharges gaged, the relation $Q=f(H-H_0)$ is very sensible.

The discharge of the stream gagings realized the 16/09/2011 and the 25/06/2013 were estimated at 0 m³.s⁻¹ because the stream wasn't enough strong to led a rotation of the propeller of the current-meter. However, the discharge wasn't really null.

Awaiting new stream gagings, we will propose the following calibration curve for the resurgence of Palestina (Fig. 16):

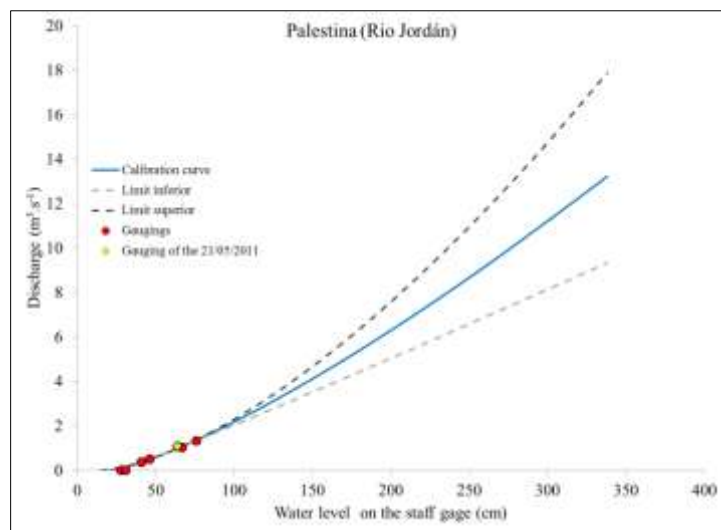


Figure 16: New calibration curve of the resurgence of Palestina (Río Jordán)

1.1.3. Monitoring of the hydrogeochemical tracers

In addition to the continuous monitoring, a regular sampling of both resurgences is realized. Samples of water of 600 mL are collected twice a month (the 1st and the 16th) by the HYBAM observer at the level of the staff gauge to monitor the following elements (Appendix 1):

- The physical chemistry parameters: pH and conductivity measured at the UNALM (Universidad Nacional Agraria de la Molina) in Lima (Peru)
- The cations (Ca^{2+} , Mg^{2+} , Na^+ , K^+) analyzed at the Geosciences Environment Toulouse laboratory (France) by ICP-OES (Inductively Coupled Plasma-Optical Emission Spectroscopy) in filtered samples ($0.45\mu\text{m}$)
- The anions (Cl^- , SO_4^{2-} , NO_3^- , F^-) analyzed at the Geosciences Environment Toulouse laboratory by ionic HPLC (High-Performance Liquid Chromatography) in filtered samples ($0.45\mu\text{m}$).

Chapter 3. Study of the hydrogeological behavior of the two resurgences

1. COMPARISON OF THE HYDROLOGICAL BEHAVIOR

1.1. Analysis of the flood hydrographs

Available discharge data run from the 19/05/2011 to the 07/02/2013 for the resurgence of Palestina and from the 01/08/2005 to the 30/09/2012 for the resurgence of Soloco. We choose to base our compared hydrodynamic study on the 2011-2012 hydrological year (from the 15/09/2011 to the 15/09/2012). It has to be considered that this year was very rainy at the level of the Marañon basin.

The study of the flood hydrographs of the two resurgences shows a difference of behavior (Fig. 17).

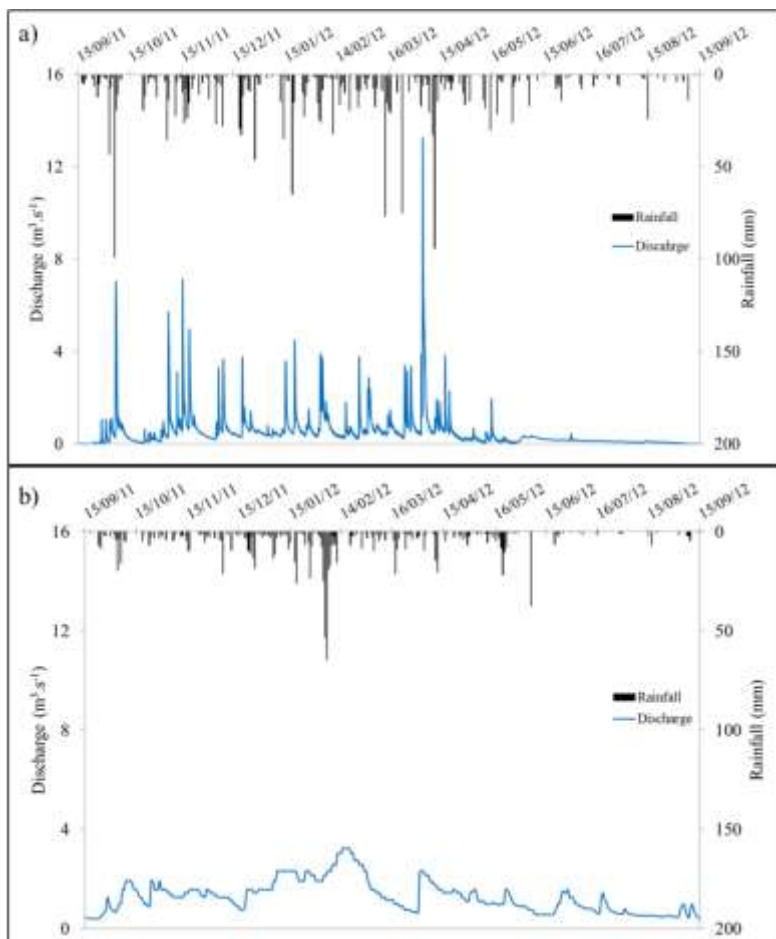


Figure 17: Flood hydrograph: a) Resurgence of Palestina; b) Resurgence of Soloco

The resurgence of Palestina presents numerous tightened flood peaks during rainy seasons (from January to April and from October to December) while these peaks are wider at the resurgence of Soloco. The lag between the beginning of the rise and the end of the decrease for Palestina is about 1-2 days, and more than 5 days for Soloco. The concentration time is also faster at Palestina (4-5 hours) than at Soloco (about 20 hours).

Moreover, we can observe that the karst of Soloco softens strongly the flood events, as the peaks never exceed $3.5 \text{ m}^3 \cdot \text{s}^{-1}$ while they are often higher than $6 \text{ m}^3 \cdot \text{s}^{-1}$ at Palestina (a peak exceeding $13 \text{ m}^3 \cdot \text{s}^{-1}$ was even registered the 14/01/2013) (Fig. 17).

This faster response of the catchment of Palestina is explained by its form more compact (K_G Palestina=1.22; K_G Soloco=1.06).

Moreover, the softening of the discharge at Soloco is explained by the distance separating the resurgence and the staff gage (see Chapter 2, §1.1.2.1.).

1.2. Correlative analysis

Correlative analysis based on the method proposed by Mangin (1984) were carried out to study the structure of the two karsts.

1.2.1. Generality and methods of analysis

1.2.1.1. *Crossed analysis*

The crossed analysis studies the correlation between the rainfall (input signal) and the discharge (output signal) and gives a view of the impulse response of the karstic system, assimilating the system to a “black box” which works as a filter.

The cross corelogram is expressed for lags k (positive or negative). In the case of poor drained systems, the response peak is smoothed, while it is more accentuated in the case of well drained systems.

1.2.1.2. *Simple analysis*

The simple analysis compares each discharge event to the previous. It allows highlighting the tendency of the karstic system to keep in memory the discharge events, looking if the information of an event comes from the previous events. This method highlights the short, mid, and long term reactions of the system in response to an input

signal. The “memory effect” of the karstic system is estimated after the simple correlogram and is equal at the number of days (k) which correspond to the value $r(k) = 0.2$. The memory effect represents the inertia of the aquifer. It gives an idea of the degree of karstification and of the water reserves (Mangin, 1984): less a system is karstified with high water reserves, slower will be the decrease of the correlogram, and higher will be the values of the memory effect and vice versa.

1.2.2. Results

The crossed analysis (time step: 1 day; truncation: 80 days) shows that the rainfall-discharge cross correlogram of the catchment of Soloco is smoother ($r=0.35$; $P=0.005$) than that of Palestina ($r=0.5$; $P=0.001$), what confirms that the rainfall signal is more filtered (Fig. 18a). It indicates a more inertial behavior for the catchment of Soloco, with a high regulation capacity.

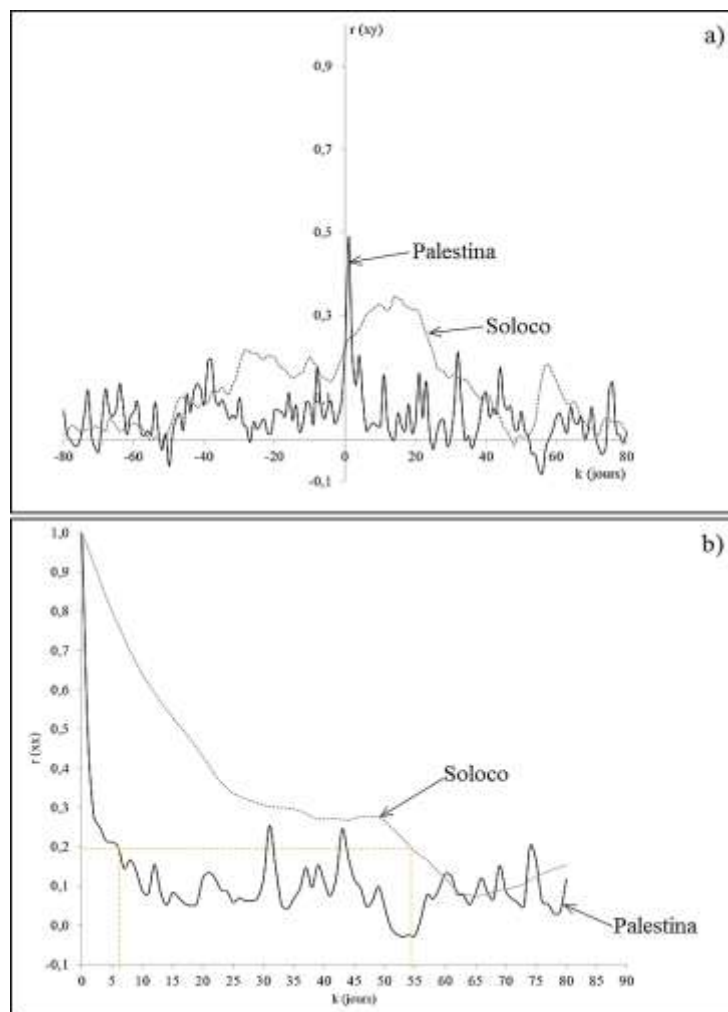


Figure 18: a) Rainfall-Discharge cross correlograms for the two resurgences; b) Discharge correlograms for the two resurgences

The simple analysis of the discharges (time step: 1 day; truncation: 80 days) (Fig. 18b) shows that the correlogram for the catchment of Palestina decreases quickly, which characterizes independent events, without memory (memory effect: 6 days). Thereby, the system of Palestina has a well-developed karstic network, with low water reserves. On the other hand, the correlogram of the catchment of Soloco decreases more slowly. It shows an important memory effect (54 days) and a regulation of the catchment by water reserves more or less important. Thus, this can translate a less advanced karstification.

During the low water period (July to September), no flood peaks are observed at the resurgence of Palestina, and the discharge decreases slowly while several rainfall events can be observed (Fig. 17). However, the rainfall events being lower during this period, we can suppose that the infiltration will be lower, what explains the absence of flood peaks. On the other hand, for the resurgence of Soloco, a few flood peaks are observed, with an augmentation of discharge overpassing $0.5 \text{ m}^3 \cdot \text{s}^{-1}$ for some peaks (Fig. 17) while few rainfall events occur during low water period.

2. GEOCHEMICAL CHARACTERIZATION OF THE RESURGENCES

2.1. Chemistry of the waters

It can be seen from Table 5 that the waters of Palestina present higher conductivity because of their higher mineralization. The temperature of water is also higher at Palestina than at Soloco due to the difference of altitude between the two resurgences. The pH of the two resurgences remains in the same order of magnitude.

Table 5: Physical chemistry parameters of the two resurgences

Resurgence	EC $\mu\text{S} \cdot \text{cm}^{-1}$	Temperature $^{\circ}\text{C}$	pH	Total Mineralization $\text{mg} \cdot \text{L}^{-1}$
Soloco	200	12.2	7.1	157
Palestina	240	19.4	7.0	221

The Figure 19 shows that, for both resurgences, the calcium and the magnesium are the major cations, accounting for 85.9% – 99.3% of the total cations, and that bicarbonates and sulfates are the major anions (81.9% - 99.8% of the total anions).

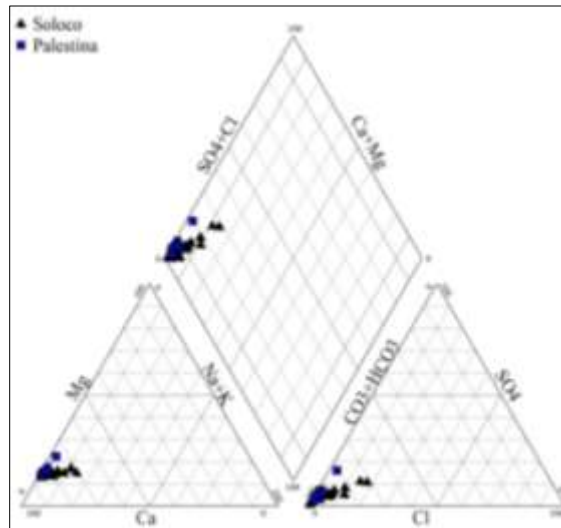


Figure 19: Piper diagram for the two resurgences

The Figure 20 is a plot of $[\text{HCO}_3^-]$ vs. $[\text{Ca}^{2+}] + [\text{Mg}^{2+}]$ and $[\text{HCO}_3^-] + [\text{SO}_4^{2-}]$ vs. $[\text{Ca}^{2+}] + [\text{Mg}^{2+}]$.

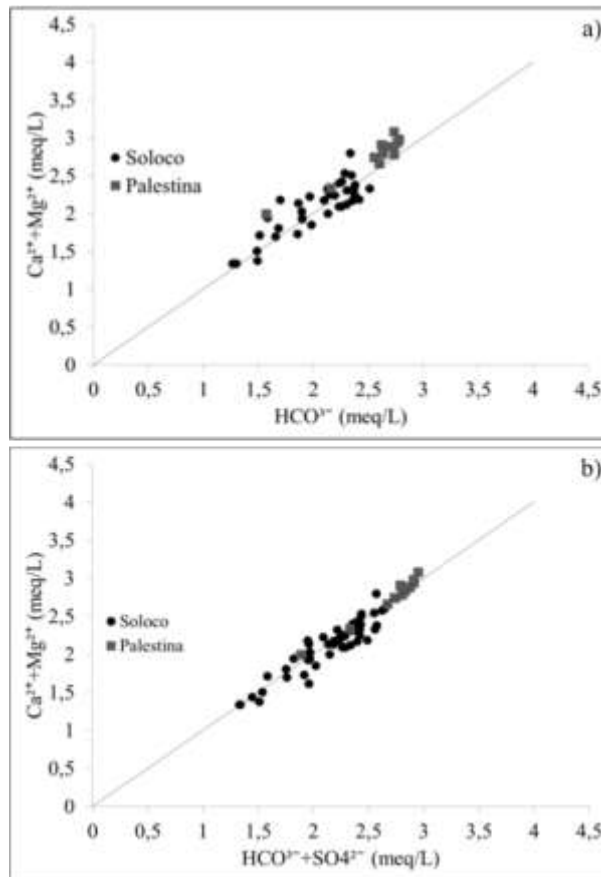
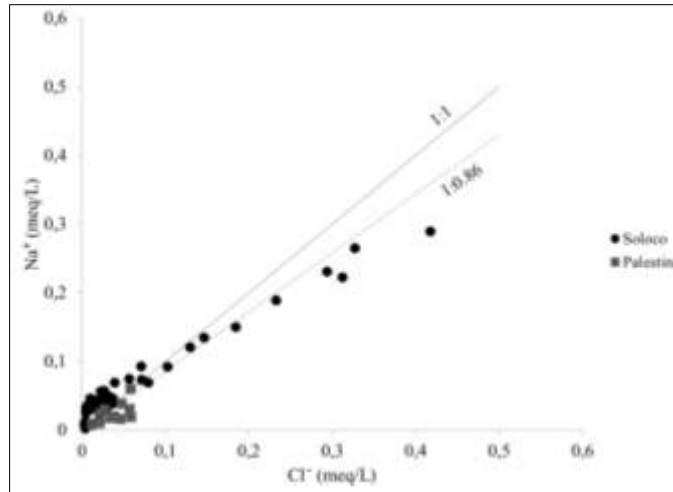


Figure 20: a) $\text{Ca}^{2+}+\text{Mg}^{2+}$ (meq/L) vs. HCO_3^- (meq/L) graph; b) $\text{Ca}^{2+}+\text{Mg}^{2+}$ (meq/L) vs. $\text{HCO}_3^- + \text{SO}_4^{2-}$ (meq/L) graph

It could be seen from Figure 20a that all the samples of the resurgence of Palestina and most of the samples of the resurgence of Soloco are located above the 1:1 line. That indicates that the dissolution of carbonates is not the only source of production of HCO_3^- , Ca^{2+} and Mg^{2+} . The Figure 20b shows that most of the samples of both resurgences are located around the equilibrium between $\text{HCO}_3^- + \text{SO}_4^{2-}$ and $\text{Ca}^{2+} + \text{Mg}^{2+}$, indicating that the dissolution of dolomites is also an important factor in the production of HCO_3^- , Ca^{2+} and Mg^{2+} in the two catchments. However, some samples of Soloco slightly fall off the 1:1 line, which could be explain by the oxidation of the pyrite present into the limestones of the Chambará formation.

The concentrations of Na^+ and Cl^- measured at the two resurgences (Fig. 21) are higher than the “theoretical” atmospheric inputs in the Marañon basin. Moquet (2011) found concentrations in Na^+ and Cl^- of rainwater around 0.005 meq/L and 0.009 meq/L.



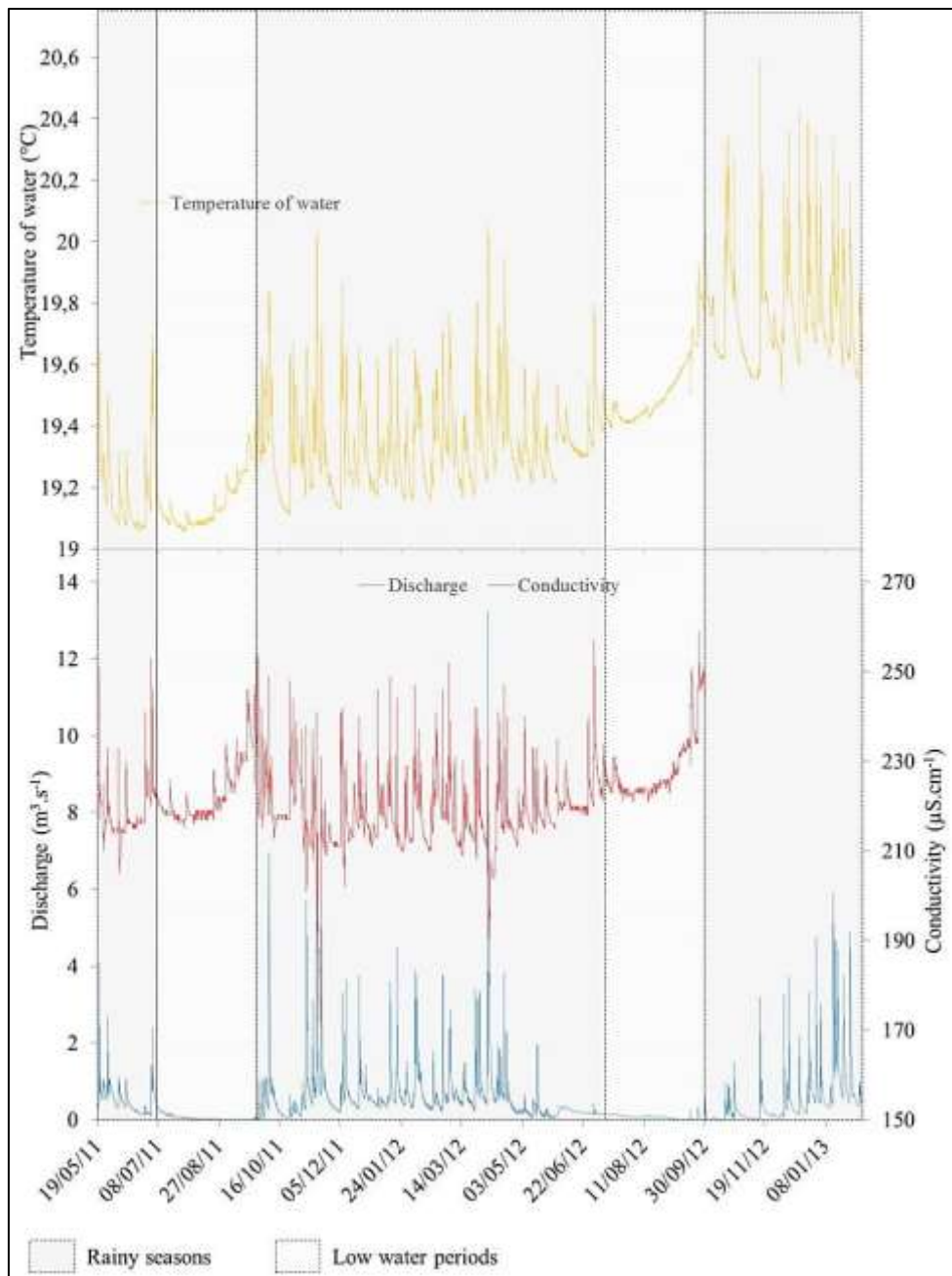


Figure 22: Temporal variation of discharge, EC and temperature of the water at the resurgence of Palestina from the 19/05/2011 to the 07/02/2013

The Figure 23 is a zoom on the flood event running from the 26/02/2012 to the 02/03/2013.

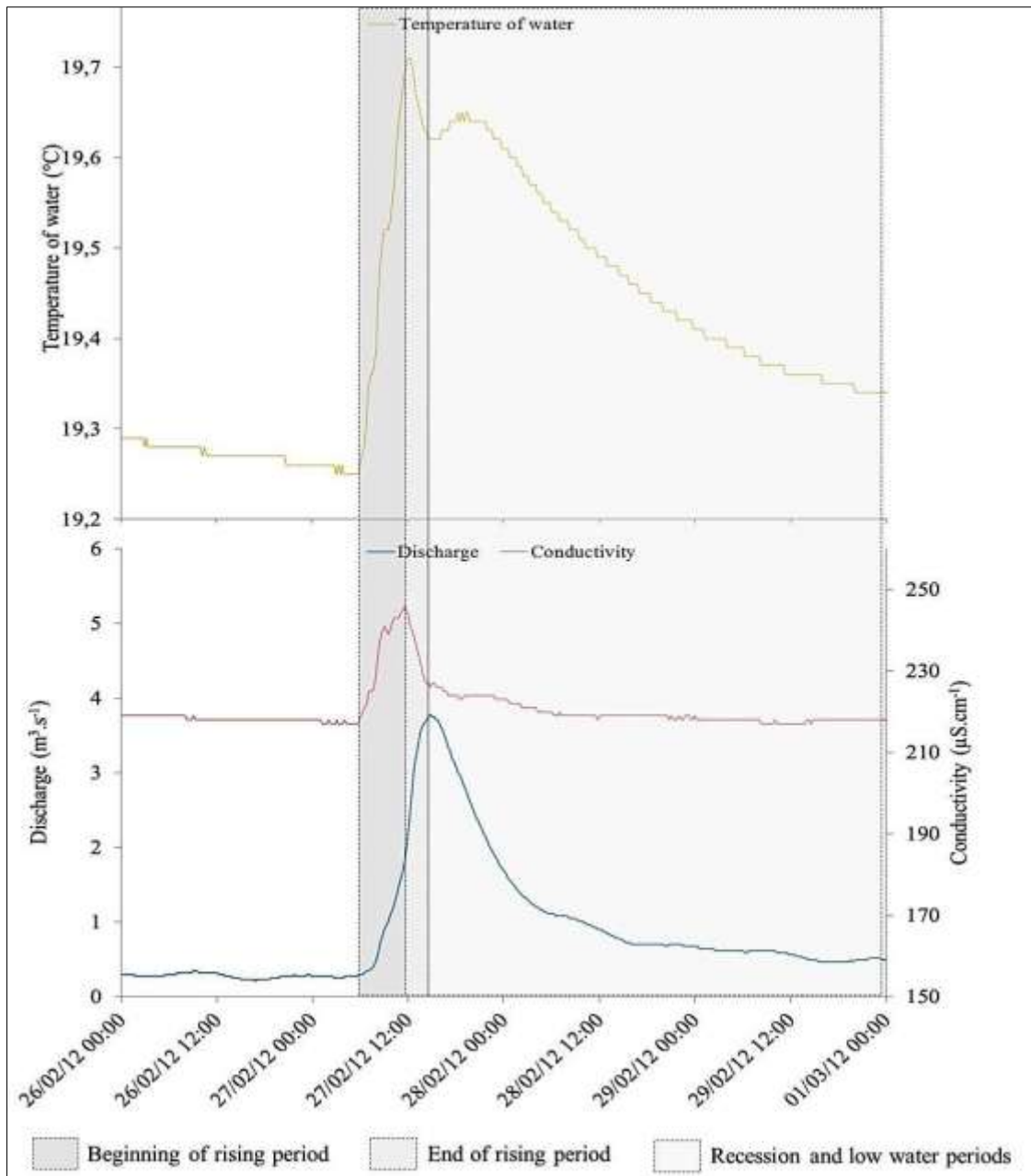


Figure 23: Zoom from the Figure 21 on the flood event running from the 26/02/2012 to the 02/03/2013

During the beginning of the rising period, a gradual increase of EC and temperature is observed as the discharge increases. The maximums of EC and temperature are reached before the flood peak, before decreasing strongly during the end of the rising period. However, the maximum of temperature is reached a little after the maximum of EC.

Recession period and low water period are marked by a slow decrease of EC and temperature as the discharge declines.

During low water period, the conductivity and the temperature get back to lower values around 230-240 $\mu\text{S}\cdot\text{cm}^{-1}$ and 19.35°C Moreover, these values tend to stabilize as the low water period persists.

With these observations, we can propose the following behavior for the resurgence of Palestina:

- An increase of the conductivity and temperature during the beginning of the rising period, corresponding to A FIRST PHASE OF THE “PISTON FLOW” WHERE MORE MINERALIZED WATERS ARE EXPELLED FROM THE FISSURED MATRIX TO THE CONDUITS.

- A sharp decrease of conductivity and temperature during the end of the recession period until the flood peak was reached, corresponding to the SECOND PHASE OF THE “PISTON FLOW” WHERE A MELTING OF HIGH MINERALIZED WATERS FROM THE SATURATED ZONE AND LOW MINERALIZED INFILTRATION WATERS FROM RAIN RUNSOFF AT THE RESURGENCE.

- A return at lower conductivity and temperature values at the beginning of the low water period which tend to stabilize as the low water period persists, INDICATING AN ALIMENTATION OF THE RESURGENCE BY THE WATERS OF THE SATURATED ZONE.

2.3. Behavior of the resurgence of Soloco

Because of a bad calibration of the CTD-Diver for the registering of the conductivity, these data could not be used. Thus, the study of the behavior of the resurgence of Soloco will be based only on the data of temperature of water registered by the CTD. These data run from the 27/05/12 to the 25/09/12 (Fig. 24). Consequently, and due to the short period cover by this registering (only 4 months), the interpretations made would be considered with caution.

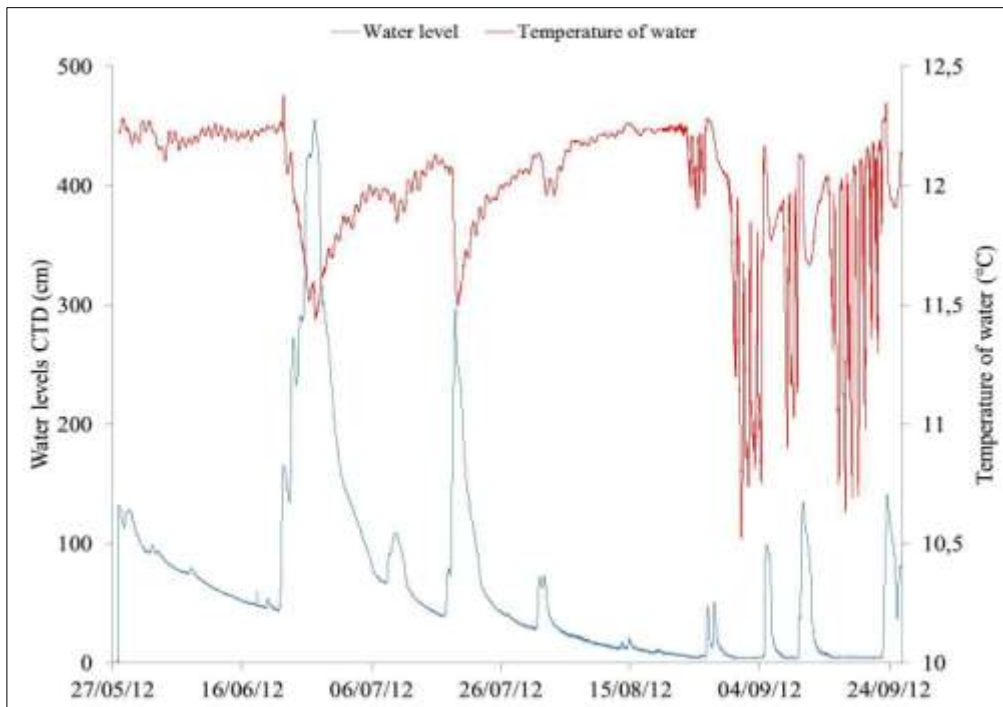


Figure 24: Temporal variation of water level and temperature of the water at the resurgence of Soloco from the 25/07/12 to the 25/09/12

Strong variations of the temperature are observed from the 27/08/2012 probably because of a malfunction of the captor.

The Figure 25 is a zoom on the flood event running from the 16/07/12 to the 31/07/12.

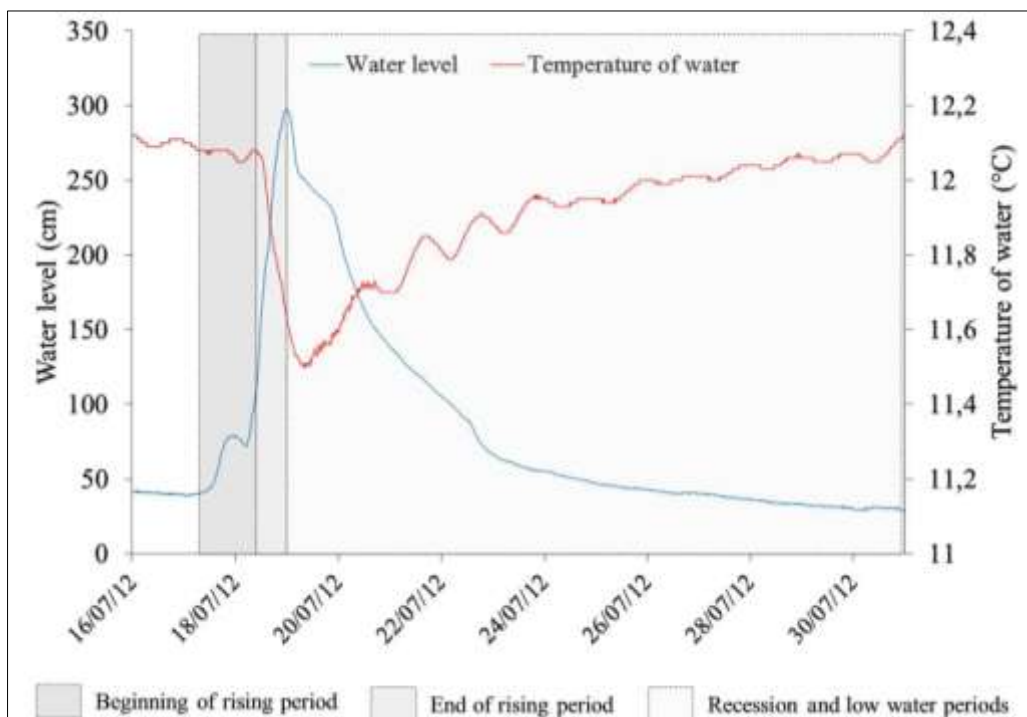


Figure 25: Zoom from Figure 23 on the flood event running from the 16/07/12 to the 31/07/12.

A very low decrease of temperature is observed during the beginning of the rising period. The temperature then decreases strongly during the end of the rising period and the beginning of the recession period. The minimum of temperature is reached after the flood peak.

During the end of the recession and the low water period, the temperature of water increases as the discharge declines, until getting back to an average value of 12.1°C at the end of the low water period

We can finally propose the following behavior for the resurgence of Soloco:

- A decrease of the temperature of water during rising period WHICH CORRESPONDS TO THE RUNOFF OF COLDER WATERS, RESULTING FROM A DILUTION EFFECT BY INFILTRATION WATERS (FROM RAIN).

- A progressive augmentation of temperature during the recession period, CORRESPONDING TO THE RUNOFF OF WARMER WATERS OF THE SATURATED ZONE.

Chapter 4. Hydrogeological contribution of the Andean calcareous massifs to the Andean tributaries of the Amazon: balance of exported dissolved solids and calculation of the karstic ablation rate for the two catchments

1. BALANCE OF EXPORTED DISSOLVED SOLIDS

We propose here to calculate the interannual average of monthly fluxes of dissolved elements exported by the two resurgences with two different methods: the HYBAM method and the M1C method proposed by Moatar et al. (2009).

The HYBAM method calculates the flux interpolating the values of concentration at discharge's time step. For the two resurgences, three values of flux were calculated with each method: one for the instantaneous discharge values, one for the minimum discharge values and one for the maximum discharge values.

The M1C method calculates the interannual average of monthly fluxes. The monthly flux is calculated using the concentration of the monthly sample multiplied by the monthly discharge of the year (see Appendix 2 for an example of calculation):

$$\boxed{F_m = \overline{C_j} \times Q_m}$$
 with: F_m : average monthly interannual flux (moles/yr)
 C_j : diary concentration
 Q_m : monthly discharge

This method is based on the hypothesis that the flux is constant for a given month.

The error associated is: $\boxed{E (\%) = \frac{\sigma(\overline{C_j} \times Q_m)}{(\overline{C_j} \times Q_m)}}$ with σ : standard deviation

The Table 6 presents the fluxes of dissolved elements calculated for Palestina and Soloco with the HYBAM and M1C methods. The flux exported by the North Peru Andean tributaries of the Amazon (High Marañon and Huallaga, HYBAM gaging stations BOR and CHA), by the Amazon in Peru at Tamshiyacu (HYBAM gaging station TAM, X=73.16°W; Y=4°S), and by the Amazon at Obidos (HYBAM gaging station OBI, X=55.51°W; Y=1.95°S) (after Moquet, 2011) are also reported in the Table.

Table 6: Interannual fluxes of dissolved elements and total dissolved solids (i.e. anions+cations+SiO₂) (TDS_{tot}) for the different stations. Catch.: name of the catchment; St.: name of the HYBAM gaging station; Per.: Period of available data; n: number of samples used to calculate the fluxes; A_{cat}: Area of the catchment; Q: interannual discharge.

Catch.	St.	Per.	n	A _{cat} km ²	Q m ³ .s ⁻¹	Method of calculation	Cl ⁻	SO ₄ ²⁻	Na ⁺	Ca ²⁺	Mg ²⁺	K ⁺	SiO ₂	HCO ₃ ⁻	TDS _{tot}
Soloco	SOL	2006-2012	48	26	1.07	HYBAM	0.07	0.21	0.05	3.35	0.14	0.03	0.13	4.12	7.60
						M1C	0.07	0.20	0.05	3.26	0.13	0.03	0.12	4.07	7.59
Palestina	PAL	2011-2012	12	15	0.5	HYBAM	0.02	0.11	0.006	1.91	0.08	0.01	0.04	2.56	4.74
						M1C	0.02	0.11	0.006	1.91	0.08	0.01	0.04	2.57	4.74
High Marañon	BOR	2003-2010	-	114.10 ³	5032 ±1138	M1C	818 ±555	1805 ±770	836 ±279	3921 ±1564	412 ±139	178 ±56	2018 ±831	12906 ±4694	23.10 ³ ±8.10 ³
Huallaga	CHA	2005-2010	-	69.10 ³	3014 ±628	M1C	2642 ±1479	1366 ±363	1955 ±1025	2966 ±728	250 ±50	119 ±30	1022 ±253	9450 ±1875	19.10 ³ ±5.10 ³
Peruvian Amazon	TAM	2003-2008	-	722.10³	28787	M1C									131.10³ ±26.10³
Total Amazon	OBI	2003-2008	-	4669.10³	174901	M1C									204.10³ ±38.10³

For the resurgence of Palestina, the fluxes calculated with both methods are similar. However, these values of fluxes must be considered with caution because the number of samples used to calculate the fluxes cover only the 2011-2012 year. Moreover, as this year was very rainy, the discharge calculated is little representative of the interannual discharge. Consequently, the fluxes calculated (at both resurgences) for this period will be overestimated.

For the resurgence of Soloco, we can observe that the results obtained with the HYBAM method are generally higher than those calculated with the MIC method. The fluxes of Ca^{2+} and HCO_3^- are those that present the higher difference.

We will consider the results obtained with the HYBAM method for the rest of the study.

Considering the TDS exported by Soloco and Palestina, and that all the limestones of the Pucará group exported dissolved elements following a homogenous dynamic, the specific fluxes of dissolved solids exported by these limestones range from 292 to 316 $\text{t.km}^{-2}.\text{yr}^{-1}$. The Andean calcareous massifs cover an area of about 24546 km^2 (Fig. 25) which represent respectively around 7.2%, 9.0% and 3.4% of the total area of the High Marañon (HYBAM gaging station BOR), of the Huallaga (station CHA) and of the Peruvian Amazon (HYBAM gaging station TAM) basins (Fig. 26 and Table 6).

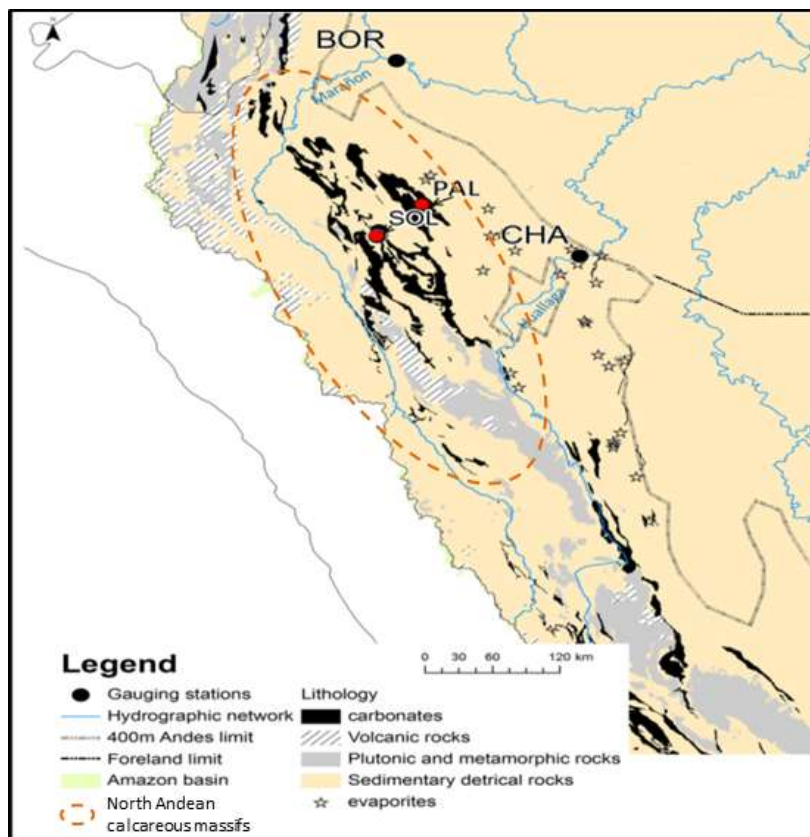


Figure 26: Localization of the Andean calcareous massifs. PAL: resurgence of Palestina; SOL: resurgence of Soloco; BOR: HYBAM gaging station of Borja; CHA: HYBAM gaging station of Chazuta (source: Moquet, 2011, modified)

If we report the specific fluxes exported by the Andean calcareous massifs to the area they cover, the average flux of total TDS they export would be about $7.5 \cdot 10^6$ t.yr⁻¹ (Table 7). This result must be considered with caution because it is calculated using only the fluxes exported by two resurgences and almost because the hypothesis made are speculative. It will have to monitor more resurgences in the future to refine this result.

Table 7: Net and relative contribution of Soloco, Palestina, and the North Andean calcareous massifs to the Marañon, the Huallaga, the Peruvian Amazon and the whole Amazon in terms of fluxes of dissolved solids and discharge. TDS_{tot}: flux of total dissolved solids (cations+anions+SiO₂); A_{lim}: surface of limestones; Q: interannual discharge.

	Balance			Relative contribution to the High Marañon (%)		Relative contribution to the Huallaga (%)		Relative contribution to the whole Amazon (%)		Relative contribution to the Peruvian Amazon (%)	
	TDS _{tot} (10 ³ t.yr ⁻¹)	A _{lim} (km ²)	Q (m ³ .s ⁻¹)	TDS _{tot}	Q	TDS _{tot}	Q	TDS _{tot}	Q	TDS _{tot}	Q
Soloco	7.6	18	1.07	0.033	0.021	–	–	0.004	0.001	0.006	0.004
Palestina	4.7	15	0.5	–	–	0.024	0.017	0.002	0.005	0.004	0.004
Calcareous massifs	7500	24546	–	32.8	–	37.9	–	3.7	–	5.7	–

This flux represents respectively 32.8%, 37.9% and 5.7% of the fluxes exported by the High Marañon, by the Huallaga and by the Amazon in Peru (station TAM) (Table 7). Compared to the flux exported by the whole Amazon (station OBI), it represents 3.7%.

These contributions are high in regard to the little surface covered by the calcareous massifs and SHOW THAT THE ALTERATION OF THESE MASSIFS CONSTITUTES ONE OF THE MAJOR SOURCE OF DISSOLVED ELEMENTS TO THE ANDEAN TRIBUTARIES OF THE AMAZON, as mentioned, among others, by Gibbs (1972), Stallard and Edmond (1983), Probst et al. (1994).

2. CALCULATION OF THE KARSTIC ABLATION RATE

The ablation rates of the karsts of Palestina and Soloco (Table 8) were calculated with the following method:

- We determined first the fluxes of Calcium exported by the resurgence (in t.yr⁻¹). For both resurgences, we made the hypothesis that all the Calcium comes from the limestones (CaCO₃). Consequently, we considered that 1 mol.yr⁻¹ of Ca²⁺ equals 1 mol.yr⁻¹ of CaCO₃ (or 100.086 g.yr⁻¹ of CaCO₃);

- Then, considering the area A covered by the limestone (in km²) inside the catchment, we calculated the unitary flux of Calcium exported at the resurgence (in t.km⁻².yr⁻¹);
- Finally, using an apparent density D of 2.7 t.m⁻³ and a total porosity of 6% for the limestones, we estimated the theoretical thickness of limestones (in mm) weathered per millenary.

Table 8: Ablation rate of the two catchments studied. V_{CaCO_3} : volume of CaCO₃ eroded (average interannual); $A_{lim.}$: area cover by the limestones of the Pucara formation.

	Ca^{2+} 10 ³ t.yr ⁻¹	V_{CaCO_3} m ³ .yr ⁻¹	$A_{lim.}$ km ²	Karstic ablation rate mm.Kyr ⁻¹
Soloco	3.14	1164	18	70
Palestina	1.91	709	15	53

The karstic ablation rate is about 70 mm.Kyr⁻¹ for the karst of Soloco, and about 53 mm.Kyr⁻¹ for the karst of Palestina.

These values CONFIRM A TREND WHICH SHOWS THAT, AT A GLOBAL SCALE, THE ANNUAL RUNOFF IS THE MAIN CONTROL FACTOR OF THE KARSTIC AB- LATION (Fig.27).

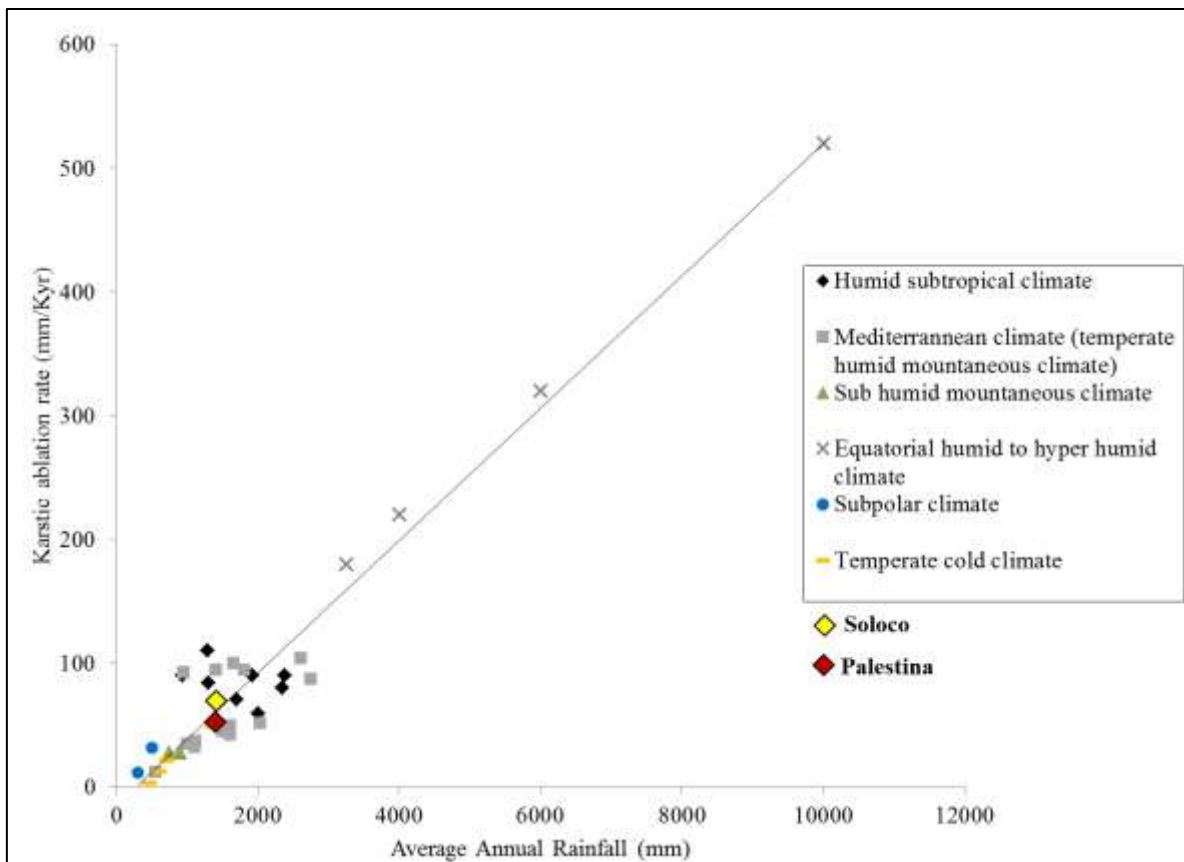


Figure 27: Karstic ablation rate for different climatic contexts according to annual rainfall

This implicates that the variations of climate (almost the rainfall) will have a direct impact on the variation of the ablation of these mediums at a brief scale. Moreover, the karsts being a major source of elements (Ca^{2+} and HCO_3^- notably) at the global scale, the climatic variations could have an impact on the cycle of these elements and on the short term's cycle of Carbon.

However we observe that, for an annual rainfall of the same order of magnitude (1372 $\text{mm}\cdot\text{yr}^{-1}$ at Soloco and 1400 $\text{mm}\cdot\text{yr}^{-1}$ at Palestina), the values of the karstic ablation are different. THAT SHOWS THAT, AT THE SCALE OF THE CATCHMENT, THE ANNUAL RAINFALL IS NOT THE ONLY FACTOR CONTROLLING THE ABLATION.

Chapter 5. A first overview of the hydrogeology of the massif of the Alto Mayo

This chapter presents briefly a first overview of the hydrogeology of the whole massif of the Alto Mayo. The informations presented in this section are the result of the investigations and measures led during the second HYBAM-PALEOTRACES field campaign which took place between the 23/06/2013 and the 13/07/2013. The aims of this campaign were to:

- Recuperate the HYBAM observer's water levels and samples at Palestina to follow the monitoring of the resurgence.

- Explore the massif of the Alto Mayo, and notably the zone of Aguas Claras y Aguas Verdes located at the north, to find new caves and resurgences (Fig. 27). The search of new caves was led in the aim to prepare the speleological expedition of the GSBM in September 2013.

- Realize stream gagings, measure the conductivity and temperature and sampled the waters of the new resurgences found and of the resurgences yet known, in order to obtain a first overview of the discharges and fluxes of dissolved solids exported at the scale of the whole massif.

1. METHODS

The conductivity and temperature of water were measured using a field conductimeter ECTestr11+. The resurgences were sampled using plastic bottles of 625 mL. No treatment of the samples (acidification, filtration,...) was made during the field campaign. The discharge was measured using three methods, according to the configuration (see Appendix 3 for a description of each method):

The realization of a complete stream gaging using an OTT C31 propeller-type current meter;

The realization of a partial stream gaging using an OTT C31 propeller-type current meter;

The use of floaters.

2. RESULTS

2.1. Hydrology and physical chemistry monitoring of the resurgences

The results of all the measured lead are presented in the Table 9.

Table 9: Values of discharge, electrical conductivity and temperature of water of all the resurgences monitored during the HYBAM-Paleotracas field campaign of June-July 2013. Res.: name of the resurgence; Lat.: Latitude; Long.: Longitude; Alt.: Altitude; H: water level on the staff gage when the stream gaging was realized; Q: discharge; EC: Electrical conductivity; T: Temperature of water.

Res.	Date	Lat.	Long.	Alt. (m)	H (cm)	Q (m ³ .s ⁻¹)	Method	EC (μS.cm ⁻¹)	T (°C)	Comments
Palestina	25/06/13	5.9258°S	77.3507°W	870	31	0	Complete stream gaging	244	20	Discharge estimated at 0 m ³ .s ⁻¹ (see Chapter 1, §1.1.2.2. for the explication)
	30/06/13				67	1.02	-	288	19.1	Discharge estimated after the calibration curve. Measure made in the afternoon after a rainfall event which has lasted all the night and the morning
Tioyacu	26/06/13	5.9985°S	77.2854°W	920	-	n.m.	-	237	17.8	Discharge no measured due to a failure of battery of the current-meter
	08/07/13				-	2.5	Complete stream gaging	241	17.7	Measure made after the pumps located downstream the resurgence were stopped
Tigre Perdido	27/06/13	5.8539°S	77.4166°W	1000	-	0.1	Partial stream gaging	275	18.9	
Campo Amor	28/06/13	5.9284°S	77.3307°W	900	-	n.m.	-	424	20.4	No flow observed at the resurgence. Conductivity and temperature measured in a pond
Palacio del Rey	28/06/13	5.85128°S	77.39378°W	930	-	0.565	Complete stream gaging	332	19.7	
Rio Negro	02/07/13	6.0891°S	77.2573°W	950	-	8.5	Partial stream gaging	299	16.4	Measure made in the afternoon after a rainfall event which has lasted all the night
Rio Aguas Claras	04/07/13	5.72514°S	77.57758°W	958	-	3.29	Complete stream gaging	289	17.7	

Waters of all the resurgences monitored present globally values of EC and temperature of the same order of magnitude excepted for Campo Amor which presents an EC of $414 \mu\text{S}\cdot\text{cm}^{-1}$ and Rio Negro whose temperature of water was 16.4°C .

The measure at Campo Amor was made in stagnant water, in a pound, what explains the higher value of EC found. For the Rio Negro, the measure was made when the resurgence was in a flood period, after a rainfall event that lasted all the night. This value of temperature remains very inferior according to those of the others resurgences. It would be interesting to follow the monitoring of this resurgence to see if the temperature of the water always remains in this order of magnitude or if it was only due to the flood event.

A first estimation of the TDS exported by each resurgence was carried out using the values of EC measured. It can be seen from Figure 28 that it exists a relation between the EC measured and the TDS both at Soloco and Palestina:

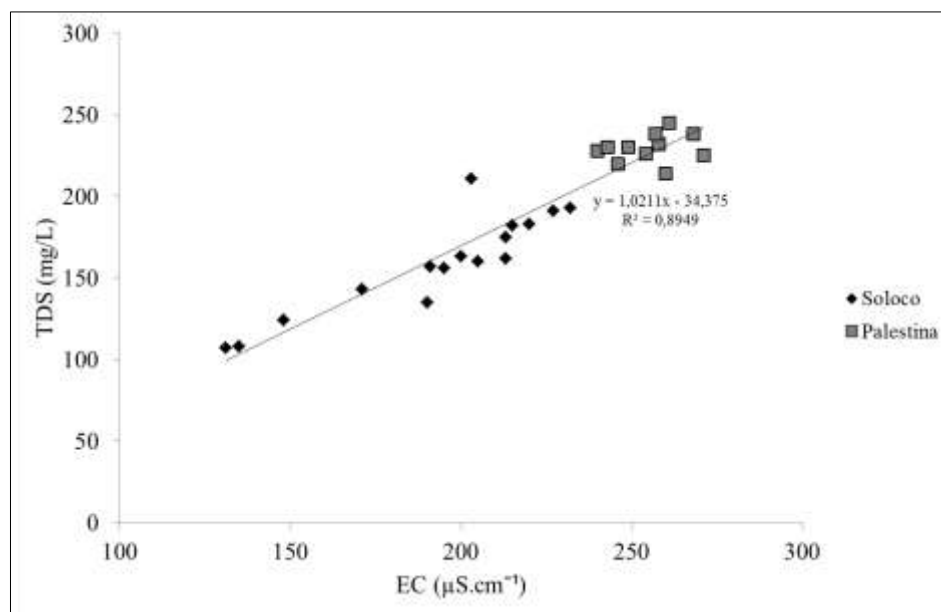


Figure 28: relation between the EC measured and the TDS at Soloco and Palestina

Considering this relation, and the fact that all the resurgences studied during the HYBAM-PALEOTRACES field campaign of June 2013 export dissolved elements following the same dynamic than Palestina, we calculated the TDS exported by all these resurgences (Table 10)

Table 10: estimation of the TDS exported by the resurgences monitored during the HYBAM-PALEOTRACES field campaign of June-July 2013. Res.: name of the resurgence; Lat.: Latitude; Long.: Longitude; Alt.: Altitude; EC: Electrical conductivity; TDS: Total dissolved solids

Res.	Date	Lat.	Long.	Alt. (m)	EC ($\mu\text{S}\cdot\text{cm}^{-1}$)	TDS ($\text{mg}\cdot\text{L}^{-1}$)
Palestina	25/06/13	5.9258°S	77.3507°W	870	244	215
	30/06/13				288	260
Tioyacu	26/06/13	5.9985°S	77.2854°W	920	237	208
	08/07/13				241	212
Tigre Perdido	27/06/13	5.8539°S	77.4166°W	1000	275	246
Campo Amor	28/06/13	5.9284°S	77.3307°W	900	424	399
Palacio del Rey	28/06/13	5.85128°S	77.39378°W	930	332	305
Rio Negro	02/07/13	6.0891°S	77.2573°W	950	299	271
Rio Aguas Claras	04/07/13	5.72514°S	77.57758°W	958	289	261

These first estimations of the TDS must be considered with a lot of caution as they are based on speculative hypothesis. The analysis of the samples collected during the field campaign will allow to confirm or disconfirm these values.

2.2. Speleological exploration

At the end of the field campaign, 13 caves were discovered, almost in the sectors of Aguas Verdes and Aguas Claras (Table 11 and Appendix 4). For more readability, the kmz file presenting the resurgences and the caves of the HYBAM-PALEOTRACES field campaign of June-July 2013 could be downloaded with the following link: <https://docs.google.com/file/d/0B8XSvjqUTVCKSjg0bHRkdzNEZDQ/edit?usp=sharing>

Table 11: caves found during the HYBAM-PALEOTRACES field campaign of June-July 2013

Cave	Date	X	Y	Altitud (m)
Bellavista	29/06/2013	77.40000°W	5.90718°S	1450,0
Cave 1 Palacio del Rey (PR1)	02/07/2013	77.39401° W	5.85595°S	918,0
Cave 2 Palacio del Rey (PR2)	02/07/2013	77.39477°W	5.85430°S	943,0
Cave 1 Aguas Claras (AC1)	04/07/2013	77.57816°W	5.77301°S	1119,0
Cave 2 Aguas Claras (AC2)	04/07/2013	77.57918°W	5.72708°S	1016,0
Cave 3 Aguas Claras (AC3)	05/07/2013	77.57230°W	5.73560°S	1194,0
Cave 4 Aguas Claras (AC4)	05/07/2013	77.57128°W	5.73272°S	1171,0
Cave 5 Aguas Claras (AC5)	05/07/2013	77.56975°W	5.73214°S	1072,0
Cave 6 Aguas Claras (AC6)	05/07/2013	77.56327°W	5.73443°S	984,0
Cave 7 Aguas Claras (AC7)	05/07/2013	77.56111°W	5.73552°S	1111,0
Cave Fabrica de Cemento (CFC)	06/07/2013	77.28447°W	6.01197°S	935,0
Cave1 Aguas Verdes (AV1)	07/07/2013	77.63298°W	5.69012°S	1155,0
Cave 2 Aguas Verdes (AV1)	07/07/2013	77.64021°W	5.69204°S	1270,0

CONCLUSION

This first study of the hydrology and hydrochemistry of the North Peruvian karsts allowed to highlight, on one hand, the difference of behavior of the resurgences of Palestina and Soloco and, on other hand, the contribution of the karsts to the Andean tributaries of the Amazon River in terms of fluxes of dissolved elements.

The analysis of the flood hydrographs and of the correlograms showed that the rainfall signal is well restituted and that the memory effect is low (6 days) for the system of Palestina, indicating a well-drained system with low water reserves. The system of Soloco presents a more inertial behavior with a rainfall signal more filtered and an important memory effect (54 days) traducing a high regulation of the karstic system by important water reserves.

The study of the geochemistry showed that the composition of the groundwater of the two karsts is mainly controlled by the weathering of the rocks forming the catchments. Waters of both resurgences have relative high conductivity and pH and are calcium bicarbonate type, indicating an impact of dissolution of carbonates rocks. Ca^{2+} , Mg^{2+} , HCO_3^- and SO_4^{2-} are respectively the main cations and anions, indicating that the dissolution of limestones and dolomites is the main factor controlling the geochemistry of groundwaters. The concentrations in Na^+ and Cl^- abnormally high could result from anthropogenic activities. The behavior of the resurgence of Palestina is of type “piston flow”, with an expelling of the waters of the saturated zone during flood events. Conversely, a dilution of the waters of the saturated zone by infiltration waters is observed at Soloco during flood events. At the scale of the High Marañon catchment, the calcareous massifs export each year about $7500 \cdot 10^3$ tons of dissolved material and contribute respectively to about 33% and 38% of the flux exported by the High Marañon and the Huallaga and confirm that the alteration of limestones is a major source of dissolved elements to the Amazon River. The values of ablation rate calculated for the karsts of Soloco and Palestina (respectively $65 \text{ mm} \cdot \text{Kyr}^{-1}$ and $47 \text{ mm} \cdot \text{Kyr}^{-1}$) are lower than those of the others tropical karsts, due mainly to a less abundant rainfall. They illustrated well the fact that, although the annual rainfall is similar for the two catchments, they respond differently in term of erosion. However, these values of ablation confirm a global trend showing that the annual rainfall is the main factor controlling the ablation.

The pursuit of the monitoring of these two resurgences, as well as the equipment of new resurgences will be necessary to follow this study, in order to better characterize the fluxes dissolved elements exported by the North Peruvian karsts.

BIBLIOGRAPHY

- Armijos Cardenas E.N., Crave A., Vauchel P., Fraizy P., Santini W., Moquet J.S., Arevalo Flores N., Carranza Valle J.L., Guyot J.L. (2013). Suspended sediment dynamics in the Amazon River of Peru. *Journal of South American Earth Sciences*, 44: 75-84.
- Auler, A., 1998. Base-level changes inferred from cave paleoflow analysis in the Lagoa Santa karst, Brazil. *JOURNAL OF CAVES AND KARST STUDIES* 60, 58–62.
- Auler, A., 1994. Hydrogeological and Hydrochemical Characterization of the Matozinhos-Pedro Leopoldo Karst, Brazil (Thesis). Western Kentucky University.
- Callède J., Cochonneau G., Ronchail J., Alves F.V., Guyot J.L., Guimarães V.S., De Oliveira E. (2010). Les apports en eau de l'Amazonie à l'Océan Atlantique. *Revue des Sciences de l'Eau*, 23(3): 247-273.
- CESPE, ECA, GSBM., 2006. Expedición Espeleológica Franco-Peruana Chachapoyas 2004 & Soloco 2005. *Bulletin Hors-série du GSBM* 102 p.
- CESPE, GBPE, GSBM, 2004. « Expédition Spéléologique Pucara 2003 » (*Bulletin Hors-série du GSBM, Spécial Pucara 2003*).
- CESPE, GBPE, GSBM., 2004. Expédition Spéléologique Pucara 2003. *Bulletin Hors-série du GSBM, Spécial Pucara 2003* 1, 70 p.
- Crowther, J., 1989. Groundwater chemistry and cation budgets of tropical karst outcrops, Peninsular Malaysia, I. Calcium and magnesium. *Journal of Hydrology* 107, 169–192.
- Cruz, F., Wang, X., Auler, A., Vuille, M., Burns, S., Edwards, L., Karmann, I., Cheng, H., 2009. Orbital and Millennial-Scale Precipitation Changes in Brazil from Speleothem Records, in: Vimeux, F., Sylvestre, F., Khodri, M. (Eds.), *Past Climate Variability in South America and Surrounding Regions, Developments in Paleoenvironmental Research*. Springer Netherlands, pp. 29–60.
- Cruz Jr., F.W., Burns, S.J., Jercinovic, M., Karmann, I., Sharp, W.D., Vuille, M., 2007. Evidence of rainfall variations in Southern Brazil from trace element ratios (Mg/Ca and Sr/Ca) in a Late Pleistocene stalagmite. *Geochimica et Cosmochimica Acta* 71, 2250–2263.
- Cruz Jr., F.W., Karmann, I., Magdaleno, G.B., Coichev, N., Viana Jr., O., 2005. Influence of hydrological and climatic parameters on spatial-temporal variability of fluorescence intensity and DOC of karst percolation waters in the Santana Cave System, Southeastern Brazil. *Journal of Hydrology* 302, 1–12.
- Cruz Jr., F.W., Karmann, I., Viana Jr., O., Burns, S.J., Ferrari, J.A., Vuille, M., Sial, A.N., Moreira, M.Z., 2005. Stable isotope study of cave percolation waters in subtropical Brazil: Implications for paleoclimate inferences from speleothems. *Chemical Geology* 220, 245–262.
- ECA, CESPE, GSBM, 2006. « Expedición Espeleológica Franco-Peruana Chachapoyas 2004 & Soloco 2005 » (*Bulletin Hors-série du GSBM*).
- ECA, GSBM, 2008. « Expedición Espeleológica Franco-Peruana Chaquil 2006 & Santiago 2007 » (*Bulletin Hors-série du GSBM*).
- Eraso, A., del Carmen DOMÍNGUEZ, M., AYUB, S., 2001. Aplicación del Método de Predicción de las Direcciones Principales de Drenaje Subterráneo al Karst de la Región de Torotoro (Bolivia), in: *13th International Congress of Speleology, Session*. pp. 20–24.
- Espinoza Villar, J.C., Ronchail, J., Guyot, J.L., Cochonneau, G., Naziano, F., Lavado, W., De Oliveira, E., Pombosa, R., Vauchel, P., 2009. Spatio-temporal rainfall variability in the Amazon basin countries (Brazil, Peru, Bolivia, Colombia, and Ecuador). *International Journal of Climatology* 29, 1574–1594.
- Gibbs, R.J., 1972. Water chemistry of the Amazon River. *Geochimica et Cosmochimica Acta* 36, 1061–1066.

- Gondwe, B.R.N., Lerer, S., Stisen, S., Marín, L., Rebolledo-Vieyra, M., Merediz-Alonso, G., Bauer-Gottwein, P., 2010. Hydrogeology of the south-eastern Yucatan Peninsula: New insights from water level measurements, geochemistry, geophysics and remote sensing. *Journal of Hydrology* 389, 1–17.
- Guyot J.L., Lavado Casimiro W.S. (2004). Caractéristiques climatiques et hydrologiques de la région = Características climáticas e hidrológicas de la región. *Bulletin du Groupe Spéléologique Bagnols Marcoule, Hors série spécial Pucara 2003*: 61-65.
- Guyot J.L. (2006). Hydro-climatologie du massif de Soloco = Hidro-climatología del macizo de Soloco. *Bulletin du Groupe Spéléologique Bagnols Marcoule, Hors série spécial Chachapoyas 2004 & Soloco 2005*: 86-89.
- Guyot J.L., Bazán Córdova H., Fraizy P., Ordoñez Gálvez J.J., Armijos Cardenas E.N., Laraque A. (2007). Suspended sediment yields in the Amazon basin of Peru : a first estimation. *Water quality and sediment behaviour of the future : predictions for the 21st century* (Webb B.W., De Boer D., Eds.), IAHS, Wallingford (Royaume Uni), 314: 3-10.
- Han, G., Liu, C.-Q., 2004. Water geochemistry controlled by carbonate dissolution: a study of the river waters draining karst-dominated terrain, Guizhou Province, China. *Chemical Geology* 204, 1–21.
- Han, G., Tang, Y., Xu, Z., 2010. Fluvial geochemistry of rivers draining karst terrain in Southwest China. *Journal of Asian Earth Sciences* 38, 65–75.
- Karmann, I., Cruz Jr., F.W., Viana Jr., O., Burns, S.J., 2007. Climate influence on geochemistry parameters of waters from Santana-Pérolas cave system, Brazil. *Chemical Geology* 244, 232–247.
- Li, S.-L., Liu, C.-Q., Li, J., Lang, Y.-C., Ding, H., Li, L., 2010. Geochemistry of dissolved inorganic carbon and carbonate weathering in a small typical karstic catchment of Southwest China: Isotopic and chemical constraints. *Chemical Geology* 277, 301–309.
- Liu, B., Liu, C.-Q., Zhang, G., Zhao, Z.-Q., Li, S.-L., Hu, J., Ding, H., Lang, Y.-C., Li, X.-D., 2013. Chemical weathering under mid- to cool temperate and monsoon-controlled climate: A study on water geochemistry of the Songhuajiang River system, northeast China. *Applied Geochemistry* 31, 265–278.
- Mangin, A., 1984. Pour une meilleure connaissance des systèmes hydrologiques à partir des analyses corrélatrice et spectrale. *Journal of Hydrology* 67, 25–43.
- Meybeck, M., 2003. 5.08 - Global Occurrence of Major Elements in Rivers, in: Editors-in-Chief: Heinrich D. Holland, Karl K. Turekian (Eds.), *Treatise on Geochemistry*. Pergamon, Oxford, pp. 207–223.
- Miller, T., 1983. Hydrology and hydrochemistry of the Caves Branch karst, Belize. *Journal of Hydrology* 61, 83–88.
- Moatar, F., Birgand, F., Meybeck, M., Fauchoux, C., Raymond, S., 2009. Incertitudes sur les métriques de qualité des cours d'eau (médianes et quantiles de concentrations, flux, cas des nutriments) évaluées à partir de suivis discrets. *La Houille Blanche* 68–76.
- Moquet, J.-S., Crave, A., Viers, J., Seyler, P., Armijos, E., Bourrel, L., Chavarri, E., Lagane, C., Laraque, A., Casimiro, W.S.L., Pombosa, R., Noriega, L., Vera, A., Guyot, J.-L., 2011. Chemical weathering and atmospheric/soil CO₂ uptake in the Andean and Foreland Amazon basins. *Chemical Geology* 287, 1–26.
- Moquet, J.-S., 2011. Caractérisation des flux d'altération des contextes orogéniques en milieu tropical - Cas des bassins andins et d'avant-pays de l'Amazone (Thèse de doctorat). Université de Toulouse III-Paul Sabatier.
- Peña, L., 2012. Las aguas subterráneas en el Perú, análisis situacional y objetivos futuros. *Revista Institucional del INGEMMET* 19.

- Probst, J.L., Mortatti, J., Tardy, Y., 1994. Carbon river fluxes and weathering CO₂ consumption in the Congo and Amazon river basins. *Applied Geochemistry* 9, 1–13.
- Stallard, R.F., Edmond, J.M., 1983. Geochemistry of the Amazon: 2. The influence of geology and weathering environment on the dissolved load. *Journal of Geophysical Research* 88, 9671.
- Steinich, B., Marín, L.E., 1997. Determination of flow characteristics in the aquifer of the Northwestern Peninsula of Yucatan, Mexico. *Journal of Hydrology* 191, 315–331.
- Vauchel, P., 2005. HYDRACCESS: Software for Management and processing of Hydro-meteorological data.
- Winter, A., Miller, T., Kushnir, Y., Sinha, A., Timmermann, A., Jury, M.R., Gallup, C., Cheng, H., Edwards, R.L., 2011. Evidence for 800 years of North Atlantic multi-decadal variability from a Puerto Rican speleothem. *Earth and Planetary Science Letters* 308, 23–28.
- Yan, J., Li, J., Ye, Q., Li, K., 2012. Concentrations and exports of solutes from surface runoff in Houzhai Karst Basin, southwest China. *Chemical Geology* 304–305, 1–9.

APPENDICES

Appendix 1:

Table of data of physical chemistry parameters and majors ions for the ensemble of the samples of the two resurgences studied

Sample	Cond	Ca ²⁺	K ⁺	Mg ²⁺	Na ⁺	HCO ₃ ⁻	Cl ⁻	SO ₄ ²⁻	F ⁻	NO ₃ ⁻	SiO ₂
	μS.cm ⁻¹	mg.L ⁻¹	mg.L ⁻¹	mg.L ⁻¹	mg.L ⁻¹	mg.L ⁻¹	mg.L ⁻¹				
Soloco 11/08/2005	213,0	36,88	0,70	4,05	1,04	128,14	0,40	4,03	n.m.	0,00	4,78
Soloco 11/09/2005	232,0	39,63	0,75	4,25	1,06	144,61	0,36	2,39	n.m.	0,00	4,96
Soloco 11/10/2005	131,0	22,57	0,46	2,57	0,76	77,49	0,30	3,07	0,00	0,00	3,07
Soloco 11/11/2005	148,0	25,54	0,61	2,77	0,67	90,92	0,32	2,50	0,02	0,22	3,17
Soloco 11/12/2005	227,0	39,58	0,60	4,04	0,78	141,56	0,22	4,08	0,03	0,50	4,16
Soloco 11/01/2006	220,0	38,35	0,60	3,96	0,89	134,24	0,31	4,32	0,03	0,54	4,12
Soloco 11/02/2006	191,0	32,76	0,52	3,67	0,73	115,93	0,17	3,09	0,02	0,00	3,87
Soloco 28/02/2006	171,0	30,68	0,50	3,35	1,14	103,12	1,14	3,33	0,02	0,00	2,92
Soloco 11/03/2006	135,0	22,81	0,54	2,44	0,60	79,32	0,20	1,88	0,00	0,00	2,92
Soloco 11/04/2006	195,0	33,41	0,53	3,19	0,57	115,93	0,17	2,62	0,02	0,00	3,44
Soloco 25/04/2006	215,0	38,72	0,43	3,88	0,79	131,80	0,20	5,61	0,03	0,53	4,08
Soloco 11/05/2006	229,0	39,05	0,95	4,04	3,01	97,97	5,02	6,41	n.m.	0,00	4,05
Soloco 11/06/2006	234,0	34,73	0,71	3,60	0,93	115,69	0,36	3,48	n.m.	0,00	3,76
Soloco 11/07/2006	201,0	40,20	0,76	4,51	3,44	145,19	6,54	9,45	n.m.	0,50	4,15
Soloco 11/08/2006	213,0	38,06	0,82	4,02	1,13	106,13	0,64	4,71	n.m.	0,00	4,14
Soloco 11/09/2006	223,0	36,09	0,81	4,08	1,29	113,75	0,89	4,70	n.m.	0,00	4,18
Soloco 11/10/2006	200,0	31,69	1,02	4,42	5,11	96,78	11,06	11,36	n.m.	1,31	3,27
Soloco 11/11/2006	188,0	32,36	0,83	3,28	1,25	91,58	0,89	1,51	n.m.	0,00	3,79
Soloco 11/12/2006	190,0	28,63	1,14	3,47	2,11	92,27	3,65	3,56	n.m.	0,04	3,57
Soloco 11/01/2007	164,0	37,47	0,64	2,90	1,43	84,00	2,37	1,87	n.m.	0,00	2,61
Soloco 11/02/2007	215,0	1,04	1,04	3,63	2,16	98,48	3,76	4,31	n.m.	0,54	3,52
Soloco 18/02/2007	218,0	39,89	0,55	3,30	0,68	97,37	0,42	2,93	0,03	0,00	2,25
Soloco 11/03/2007	203,0	36,73	n.m.	3,85	2,49	114,51	3,94	4,77	0,04	0,80	3,36
Soloco 11/04/2007	199,0	34,08	n.m.	3,49	0,86	112,05	0,76	3,21	0,05	0,00	3,07
Soloco 11/05/2007	188,0	35,51	n.m.	3,77	2,23	n.m.	3,66	2,80	3,20	0,00	3,16
Soloco 28/05/2007	223,6	36,13	2,73	4,62	6,66	103,70	14,80	12,04	0,04	0,92	2,50
Soloco 11/06/2007	248,7	43,03	0,78	4,68	2,77	139,73	4,60	7,13	0,05	0,75	3,61
Soloco 11/07/2007	246,5	42,57	1,13	4,64	2,13	143,39	2,51	4,01	0,05	0,00	3,83
Soloco 11/08/2007	275,0	46,89	2,09	5,57	5,31	142,78	10,42	11,16	0,05	2,32	4,01
Soloco 11/09/2007	238,9	40,87	0,57	4,66	1,72	137,90	2,00	6,16	0,05	0,81	3,07
Soloco 11/10/2007	224,6	38,70	0,60	4,74	1,30	129,97	0,81	4,26	0,05	0,01	3,90
Soloco 11/11/2007	220,3	37,15	0,68	4,53	3,09	120,21	5,19	5,86	0,02	0,93	3,07
Soloco 11/12/2007	236,7	40,80	0,76	4,43	1,69	136,68	2,54	5,57	0,03	0,57	3,13
Soloco 11/01/2008	191,8	27,41	0,76	3,96	4,34	101,29	8,25	4,85	0,02	0,70	3,68
Soloco 11/02/2008	192,9	29,20	0,60	3,31	0,70	113,49	0,57	2,94	0,03	1,14	3,72
Soloco 11/03/2008	246,5	37,46	2,59	3,82	1,59	147,66	2,83	3,53	0,04	0,09	4,59
Soloco 11/04/2008	221,4	36,27	0,66	3,45	0,20	136,24	0,19	1,61	0,02	n.m.	3,28
Soloco 11/05/2008	222,5	36,07	0,65	3,59	0,17	137,80	0,22	1,60	0,03	n.m.	3,25
Soloco 11/06/2008	246,5	39,85	0,68	4,14	0,28	153,57	0,16	2,19	0,03	0,44	3,63
Soloco 11/07/2008	235,6	38,19	0,69	4,16	0,30	145,07	0,16	2,16	0,03	0,47	3,66
Soloco 11/08/2008	154,6	23,22	0,61	2,66	0,05	91,05	0,14	1,02	0,02	0,12	2,43
Soloco 11/09/2008	211,5	34,03	0,68	3,64	0,14	130,27	0,13	0,75	0,02	n.m.	3,10
Soloco 11/10/2008	200,6	31,45	0,65	3,39	0,17	121,25	0,10	1,74	0,78	n.m.	3,18
Soloco 11/11/2008	226,8	36,05	0,64	3,89	0,18	140,60	0,18	1,62	0,02	0,01	3,36
Soloco 11/12/2008	231,2	36,92	0,67	3,97	0,18	143,95	0,13	1,93	0,03	n.m.	3,45
Soloco 11/05/2011	209,0	n.m.	n.m.	n.m.	n.m.	n.m.	n.m.	n.m.	n.m.	n.m.	n.m.
Soloco 11/09/2011	180,7	38,03	0,73	3,84	0,88	102,02	1,29	8,41	0,04	1,04	3,33
Soloco 11/10/2011	175,1	35,60	0,91	4,28	1,00	98,88	0,58	5,85	0,03	0,71	3,67
Soloco 11/11/2011	169,6	43,80	0,91	4,75	0,99	95,80	0,71	10,26	0,03	0,85	3,17
Soloco 11/12/2011	208,0	39,74	0,76	3,99	1,06	117,31	1,31	12,58	0,03	1,61	2,79
Soloco 11/01/2012	184,9	36,85	0,67	3,55	0,69	104,37	1,04	8,41	0,03	1,60	3,21
Soloco 11/02/2012	196,7	42,03	0,71	3,64	0,84	110,98	0,91	9,57	0,04	1,32	3,50
Soloco 11/03/2012	232,0	47,90	0,99	4,12	0,71	130,76	0,84	7,90	0,04	1,52	1,83
Soloco 11/04/2012	205,0	25,66	0,66	1,93	0,40	115,63	0,77	8,00	0,03	0,95	3,42
Soloco 11/05/2012	115,4	45,60	1,24	3,94	0,85	65,43	1,10	11,14	0,03	0,65	2,50
Soloco 11/06/2012	221,0	42,83	0,92	4,93	6,09	124,60	11,59	13,55	0,03	1,71	3,58
Soloco 11/07/2012	192,1	33,02	0,63	3,60	1,02	108,40	1,05	3,32	0,03	0,31	2,58
Soloco 11/08/2012	204,0	36,38	0,80	4,46	1,59	115,07	1,39	4,37	0,03	0,49	3,88
Soloco 11/09/2012	153,4	25,26	0,74	4,26	1,32	86,72	0,96	5,77	0,03	0,19	n.m.

Sample	Cond	Ca ²⁺	K ⁺	Mg ²⁺	Na ⁺	HCO ₃ ⁻	Cl ⁻	SO ₄ ²⁻	F ⁻	NO ₃ ⁻	SiO ₂
	μS.cm ⁻¹	mg.L ⁻¹	mg.L ⁻¹	mg.L ⁻¹	mg.L ⁻¹	mg.L ⁻¹	mg.L ⁻¹				
Palestina 05/2011	268,0	50,90	1,69	4,86	0,43	169,0	2,10	6,95	0,05	1,57	2,33
Palestina 09/2011	271,0	30,84	0,70	5,56	0,71	96,0	2,03	15,05	0,06	6,20	2,58
Palestina 10/2011	258,0	49,82	0,57	5,11	0,47	160,0	1,31	8,12	0,06	6,72	2,17
Palestina 11/2011	249,0	49,63	0,63	4,67	0,40	167,0	1,22	4,99	0,05	1,01	2,75
Palestina 12/2011	243,0	49,43	0,52	5,10	0,43	164,0	1,40	7,15	0,05	2,15	2,46
Paestina 01/2012	261,0	52,86	0,64	5,33	0,38	167,0	1,65	10,44	0,04	6,33	2,00
Palestina 02/2012	249,0	38,51	1,09	5,04	0,22	132,0	0,77	8,22	0,04	0,70	2,25
Palestina 03/2012	257,0	50,41	0,60	5,59	0,23	170,0	0,46	6,09	0,05	4,34	1,79
Palestina 04/2012	240,0	48,74	0,81	4,82	0,23	167,0	0,67	4,72	0,05	0,72	2,58
Palestina 05/2012	243,0	49,49	0,55	4,97	0,18	167,0	0,42	6,81	0,05	1,00	2,42
Palestina 06/2012	246,0	46,38	0,61	5,17	0,89	156,0	1,69	8,63	0,05	0,50	2,13
Palestina 07/2012	260,0	44,82	0,51	5,12	0,54	159,0	0,77	3,33	0,05	0,21	2,08
Palestina 08/2012	254,0	47,15	0,58	5,37	1,38	161,0	2,07	8,13	0,05	0,16	2,00
Palestina 09/2012	271,0	46,59	0,66	5,54	0,69	167,0	0,97	3,34	0,05	0,00	2,33

Appendix 2:

Example of calculation of the interannual monthly flux of Ca^{2+} (expressed in tons of CaCO_3) with the MIC method at Soloco for the 2006-2012 period. C_j : monthly concentration of the sample ($\text{mg}\cdot\text{L}^{-1}$); Q_m : monthly discharge ($\text{m}^3\cdot\text{s}^{-1}$); $F_{m_{an}}$: monthly flux for the considered year ($\text{t}\cdot\text{month}^{-1}$); F_m : average interannual flux ($\text{t}\cdot\text{month}^{-1}$); σ : interannual standard deviation of the values $F_{m_{an}}$; F_{an} : interannual flux ($\text{t}\cdot\text{yr}^{-1}$)

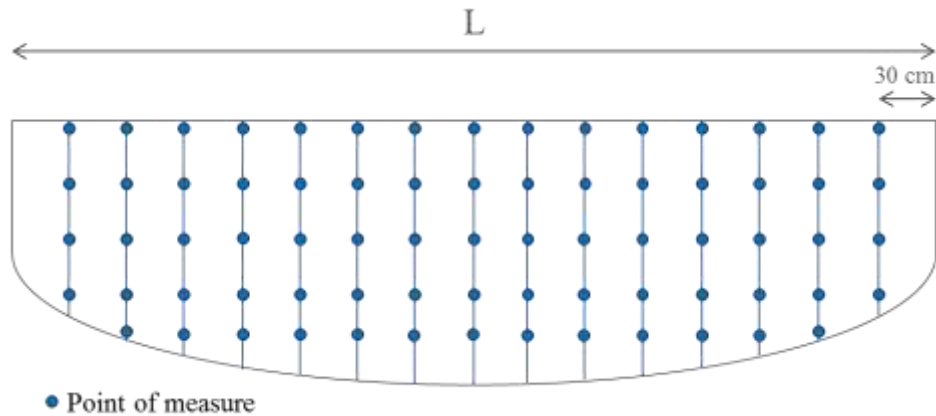
Month	Variable	Year					Fm interannual average	σ interannual
		2006	2007	2008	2011	2012		
J	C_j	92.73	93.57	71.21	94.28	95.32	373.26	67.75
	Q_m	0.85	2.93	1.32	0.52	2.09		
	$F_{m_{an}}=C_j\times Q_m$	211.6	734.33	259.20	127.32	533.84		
F	C_j	80.82	99.62	77.09	94.35	107.30	361.60	57.24
	Q_m	1.05	1.55	1.47	0.87	2.64		
	$F_{m_{an}}=C_j\times Q_m$	213.6	388.13	284.52	212.76	708.96		
M	C_j	65.92	90.81	91.72	94.44	106.00	320.56	35.62
	Q_m	2.36	1.61	1.43	0.52	1.11		
	$F_{m_{an}}=C_j\times Q_m$	416.15	392.08	351.79	128.51	314.29		
A	C_j	87.79	86.26	90.62	94.52	78.09	377.27	19.56
	Q_m	1.72	1.46	1.44	2.04	1.63		
	$F_{m_{an}}=C_j\times Q_m$	391.39	325.54	339.18	500.53	329.72		
M	C_j	94.96	89.43	92.27	94.60	109.50	305.04	28.36
	Q_m	0.69	1.72	1.14	1.32	1.13		
	$F_{m_{an}}=C_j\times Q_m$	175.24	412.47	282.48	323.91	331.12		
J	C_j	90.35	105.10	98.09	94.68	101.80	245.76	21.61
	Q_m	0.83	0.83	1.32	1.01	0.85		
	$F_{m_{an}}=C_j\times Q_m$	194.84	227.20	334.59	247.62	224.55		
J	C_j	98.43	108.80	87.02	94.77	85.66	184.79	15.85
	Q_m	0.83	0.54	0.66	0.84	0.83		
	$F_{m_{an}}=C_j\times Q_m$	217.76	157.94	151.27	206.34	190.66		
A	C_j	94.20	113.10	66.13	94.85	84.00	135.44	10.15
	Q_m	0.60	0.45	0.83	0.50	0.53		
	$F_{m_{an}}=C_j\times Q_m$	151.13	136.92	145.95	124.15	119.02		
S	C_j	87.95	101.70	82.10	93.57	63.04	147.06	26.32
	Q_m	0.64	0.49	0.76	0.83	0.60		
	$F_{m_{an}}=C_j\times Q_m$	144.53	128.38	162.58	201.79	98.04		
O	C_j	80.11	96.05	81.52	93.88	-	241.93	38.60
	Q_m	0.59	1.06	1.01	1.38	-		
	$F_{m_{an}}=C_j\times Q_m$	125.95	273.47	220.31	348.00	-		
N	C_j	78.65	95.01	89.89	106.00	-	333.86	41.41
	Q_m	0.95	2.03	1.08	1.42	-		
	$F_{m_{an}}=C_j\times Q_m$	193.67	500.17	251.17	390.42	-		
D	C_j	77.06	93.72	92.10	98.08	-	237.62	30.58
	Q_m	1.04	0.99	0.64	1.26	-		
	$F_{m_{an}}=C_j\times Q_m$	213.83	247.76	157.63	331.26	-		
F_{an}							3264.20	325.97

Appendix 3:

Description of the different methods used to calculate the discharge of the resurgences studied during the field campaign of June-July 2013

1) Complete stream gaging:

A vertical is realized each 30 cm. For each vertical, various points of measure are made. An average on 30s is realized at each measure.



The results of the stream gaging are then treated with the Hydraccess software with the module “Process the Discharge measurement” (tab “Discharge Measurement”).

2) Partial stream gaging:

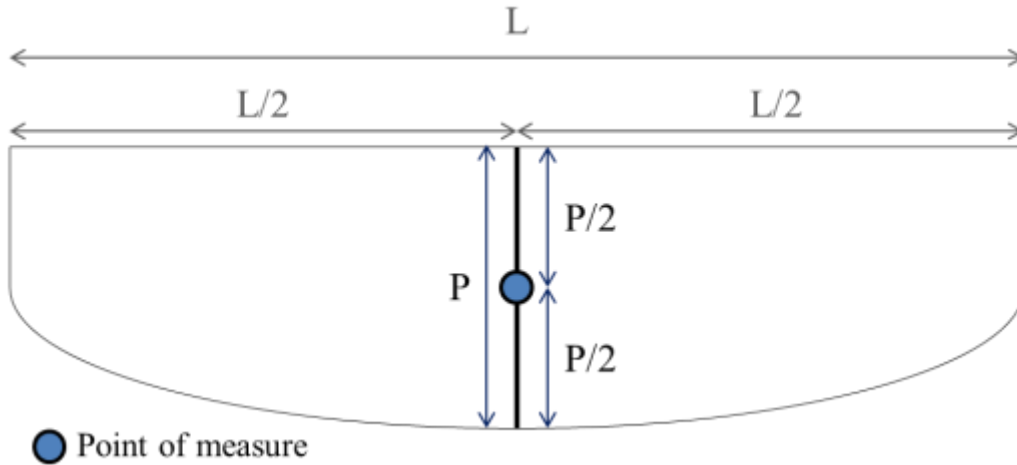
A unique measure of is realized at the middle of the river, at mid depth. The number of rotations n of the propeller of the current-meter, expressed in $1.s^{-1}$, is converted into speed (s) using the following equation:

- if $n \leq 0.70$, $s = 0.2294 \times n + 0.022$

- if $0.70 \leq n \leq 9.99$, $s = 0.2494 \times n + 0.008$

Taking the two-third of the speed, the discharge Q is calculated as following:

$$Q = \left(\frac{2}{3} \times s\right) \times L \times P \quad \text{with } L: \text{ width of the river (m); } P: \text{ depth at the middle of the river (m)}$$



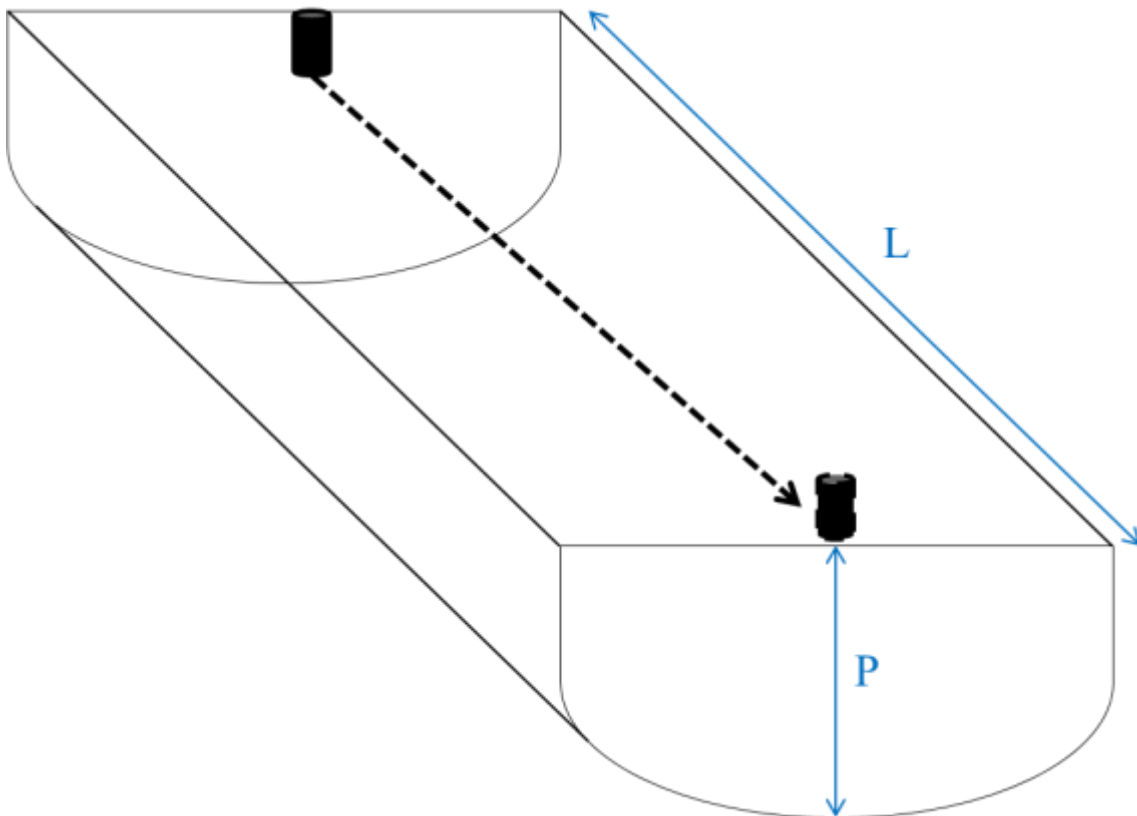
3) Estimation of the discharge using floaters:

The speed is estimated calculating the time take by a floater to cross a distance L .

Taking the two-third of the speed, the discharge Q is calculated as following:

$$Q = \left(\frac{2}{3} \times s\right) \times L \times P$$

with L : width of the river (m); P : depth at the middle of the river (m)



Appendix 4:

Map of the resurgences and caves of the HYBAM-PALEOTRACES field campaign of June-July 2013

